Republic of Iraq
Ministry of Higher Education
& Scientific Research
University of Babylon
College of Education for Pure Sciences
Department of Physics

Study the Linear and Nonlinear Optical Properties for Methylene Blue Dye Doped SiO_2 Nanoparticles

A Thesis

Submitted to Council of College of Education

for Pure Sciences, University of Babylon in Partial

Fulfillment of Requirements for the Degree

of Master in Education / Physics

By

Maha Hasan Noory Khaleel
B.Sc. in physics
University of Babylon (2010)

Supervised by

Prof. Zaid A. Hasan Al – shimary

2022 A.D **1444 A.H**

بِسۡمِ ٱللَّهِ ٱلرَّحۡمَٰنِ ٱلرَّحِيمِ

{يَرۡفَعِ ٱللَّهُ ٱلَّذِينَ ءَامَنُواْ مِنكُمۡ وَٱلَّذِينَ أُوتُواْ ٱلۡعِلۡمَ دَرَجَٰتٖۚ وَٱللَّهُ بِمَا تَعۡمَلُونَ خَبِير}

صدق الله العلي العظيم

سورة المجادلة (الآية 11)

Dedication

To my dear father.

To my beloved mother.

To my daughters.

To my brothers and sisters…

To my close friends,

To my teachers,

And

Everyone who has helped me…

Maha 

Acknowledgments

Praise be to Allah, Lord of the Worlds, and blessings and peace be upon our master Muhammad, his good, pure household, and his chosen, righteous companions.

And after.

After thanking Allah Almighty for completing this research, I cannot help but offer my sincere thanks and gratitude to the respected supervisor **Prof.Dr. Zaid A. Hasan** for his suggestion of the research topic and for his valuable advice and guidance.

The continued success of this research throughout the period of work and the preparation of the thesis.

I also thank the Dean of the College of Education for Pure Sciences and the Head of the Physics Department and all the distinguished professors of the Department of Physics for their permanent cooperation throughout the study period.

I also thank the graduate students in the Department of Physics for their cooperation and support.

Last but not least, I extend my thanks and pride to everyone who helped me.

Maha

Abstract

The (Methylene Blue dye /silicon dioxide) nanocomposites films have been prepared by casting method with different weight percentage of (SiO_2) nanoparticles.The structural, optical and nonlinear properties of nanocomposites have been studied. The structural properties include optical microscope. The examination results by photos optical microscope showed distribution of silicon oxide nanoparticle inside the methyl blue dye for all nanocomposites films, the optical microscope images also showed continuous network of ions inside the methyl blue dye at high ratio of nanoparticles. The results of optical properties for (MBD/ SiO_2) nanocomposites films showed that the absorbance, absorption coefficient, extinction coefficient, refractive index, real and imaginary dielectric constants and optical conductivity increase with the increase of the nanoparticles concentrations while the transmittance and energy band gap were decreased with increase the (SiO_2) nanoparticles concentrations.

The (MBD/SiO_2) nanocomposites have high absorbance in the UV-region. The nonlinear tests calculated used (Z - Scan) technique in two cases (Close aperture) and (Open aperture) for obtain nonlinear refractive index coefficient (n_2) and nonlinear absorption coefficient (β). The measurements performed using diode laser operating of a continuous wave (CW) at (540 nm) wavelength. The results showed a decrease both of the nonlinear refractive index coefficient and nonlinear absorption coefficient, when increasing concentrations for all samples of nanocomposites films.

The results showed the nonlinear refractive index in all samples is negative. The results showed the nonlinear absorption coefficient (β) in three cases of thin films for (MBD/ SiO_2) films with addition (1,3,5)% (gm)of (SiO_2) nanoparticle it noticed two photon absorption While the largest nonlinear absorption (Saturable absorption) noticed that in the case sample pure.

Contents

List of symbols

Symbols	Physical meaning
A	Absorbance
B	Constant depended on type of material
C	Velocity of light in vacuum
E	Electrical field intensity
$\boldsymbol{\varepsilon}$	Complex dielectric constant
$\boldsymbol{\varepsilon_0}$	Vacuum permittivity
$\boldsymbol{\varepsilon_1}$	Real part of the dielectric constant
$\boldsymbol{\varepsilon_2}$	Imaginary part of the dielectric constant
$\boldsymbol{E_{Ph}}$	Energy of phonon
$\boldsymbol{h}$	Plank constant
$\boldsymbol{h\upsilon}$	Photon energy
$\boldsymbol{I_A}$	Absorbed light intensity
$\boldsymbol{I_0}$	Incident intensity of light
$\boldsymbol{I_p}$	Conduction current
$\boldsymbol{k_0}$	Extinction coefficient
L	Polar length

N	Refraction index
N	Concentration of charge carriers
$\boldsymbol{Nlo}$	Optical inear properties
P	Total dipole moment
R	Reflectance
T	Temperature
$\boldsymbol{T_r}$	Transmittance
D	Thickness
V	Velocity of light in medium
$\boldsymbol{v}$	Frequency
$\boldsymbol{\alpha}$	Absorption coefficient
$\boldsymbol{\lambda}$	Wavelength
$\boldsymbol{\mu i}$	Electrical dipole moment
$\boldsymbol{\mu}$	Mobility of charge carriers
$\boldsymbol{\Delta k}$	Changes in wave vector

List of abbreviations

abbreviations	Meanings
SiO_2	Silicon oxide
C.B	Conduction bond
M_w	Molecular weight
MBD	Methylene Blue Dye
V.B	Valence bond

List of tables

List of Figures

1.1 Introduction

Some oxides are so dense that the controlled growth of their layers can protect the alloy or metal from further oxidation. Even studies have revealed that the oxidation of the protective layer continues as if it were a liquid covering all surface cracks or defects of the metal. Metal oxides can adopt exquisite structures, either as nanoparticles or as large polymeric aggregates. This fact makes them the subject of studies for the synthesis of smart materials, due to their large surface area, which is used to design devices that respond to the least physical stimuli. Likewise, metal oxides are the raw material for many technological applications, from mirrors and ceramics with unique properties to electronic equipment, to solar panels [1]. High surface areas help prevent particle agglomeration and also im-prove their reactivity and stability, nowadays, we note the interest in solid/ dense silica coating around metal nanoparticles to investigate their optical properties [2,3]. Nanoparticles of SiO_2 are the most manufactured material in terms of quantity among the various spectrums of nanomaterials due to its many uses in various aspects of life, and the fact that the cost of its production is often cheaper than the cost of producing most nanomaterials, in addition to its relatively easy handling compared to other nanomaterials. Also, SiO_2 [4-7]. In addition, the effect of SiO_2 nanoparticles was recently analyzed showing that most efficient epoxidation catalyst [8]. The SiO_2 films these films are transparent in the infrared field, as they are transparent with a high transmittance coefficient up to ~70% [9] Dye is a chemical compound used to produce long-lasting colors on the surface of materials. We deal with dyes in the details of our daily lives, in our clothes, food, writing supplies such as ink and paper, in utensils and furniture, plastic and many more.

Some brightly colored dyes draw our attention, and most of the time they no longer draw our attention or realize their existence, because we now deal with dyes in the details of our daily lives, in our clothes, food, writing supplies such as

ink and paper, in utensils and furniture, plastic and many more [10]. The interest in dyes was ancient due to the presence of colors in the natural environment surrounding humans, including plants, animals, stones, dust and sand.

Humans began dyeing fabrics and other materials over 5,000 years ago. Dyers have also used color-fixing chemicals for thousands of years in 1856, the English chemist William Perkin discovered the first synthetic dye. This dye called mauvy was a faint purple hue. Perkin produced this dye while trying to extract an alkaloid from a coal tar dye product called aniline [11].

Germany produced most of the world's dyes. The Germans stopped supplying other countries with dyes. As a result of this situation, the dye industry developed rapidly in many countries. Since the forties of the twentieth century, chemists have invented many industrial yarns and textiles, and they have also developed thousands of synthetic dyes suitable for these yarns [12].

Definition: A dye is a compound capable of binding in some way with the fibers to be dyed, giving them color [13]. A chemical compound gets a color when it has the ability to absorb one band of the visible spectrum and reflect the rest [14]. The appearance of color depends on a number of physical, chemical, physiological and psychological factors and the part of the spectrum that a person sees in a range of wavelengths between 400-700 nanometers [15].The perception of light occurs through the absorption of light by the atoms of the material, where it absorbs part of it and reflects another part, and it passes through the material of low density, or then the light emitted from the light source or reflected by a reflective surface begins to have a chemical effect, and the light reaches the retina of the eye. The eye, from which information is transmitted to the brain, in order to reach the so-called perception [16]

1.2 Nanomaterials

Nanomaterials (Nanometric) are: materials with a nanometer dimension confined between 1 to 100 nanometers, and nano materials exist in three forms: one-dimensional, two-dimensional and also three-dimensional [17,18] (as in Figure 1-1). Objects at the nanoscale behave completely differently than they behave at the larger scale, as gold in the large scale (BULK), for example is good heat and electricity conductor, but it is not conductor of light. Whereas, gold nanoparticles with a suitable structure absorb light, and they can convert that the light turns into sufficient heat to make it work as a small heat scalpel, through which it can kill unwanted cells in the human body, such as cells of cancer

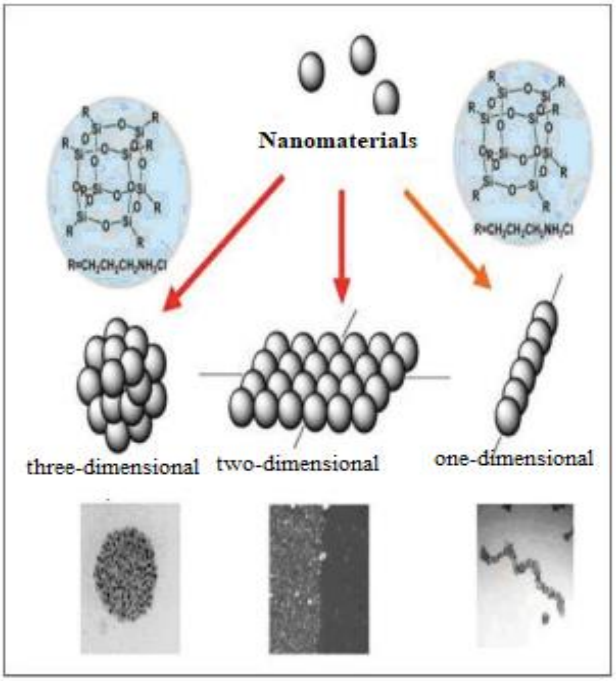

Figure (1-1): Dimensional classification of nano materials [17]

Also, some materials can become noticeably stronger, when they are built at the nanoscale. For example, we note that carbon nano tubes see (figure1-2), which they have a diameter approximately diameter 0.025 of human hair are incredibly strong, as they are used in the manufacture of baseball bats, Bicycles and car parts, and scientists are thinking of collecting carbon nanotubes from plastic to make a composite that is lighter than steel, and at the same time more powerful than it.

Energy can also be saved if we replace some of the metals used in the automobile industry with this compound. It conducts heat and electricity better than any other metal, so it can be used to protect aircraft from lightning strikes, and it can also be used in electrical computer circuits [17,18].

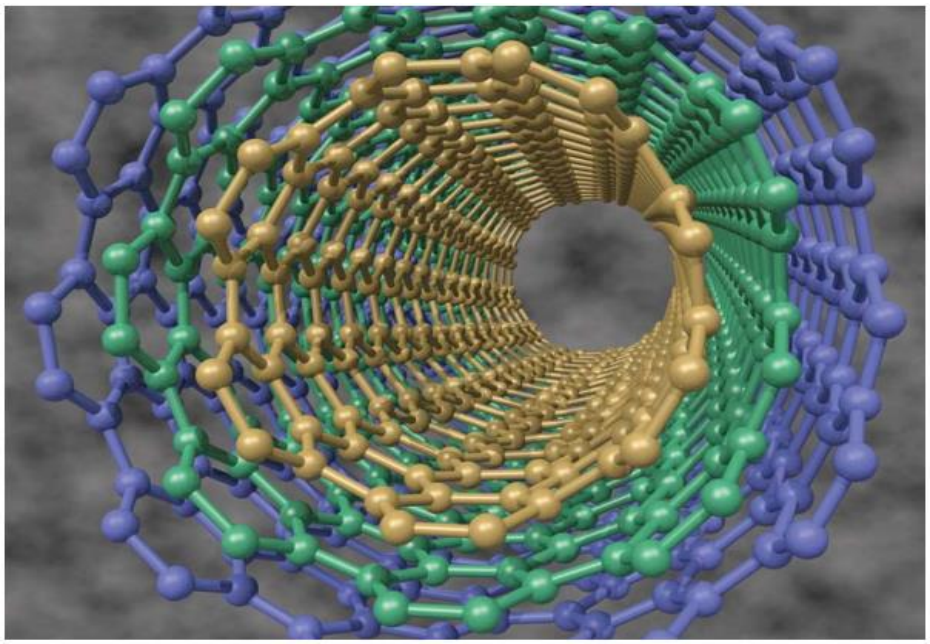

Figure (1-2): An imaginary image of a multi-walled carbon nanotube

1.3 Organic Dye

The chromophore is a part of an organic molecule formed by a group of electrons and atoms, which gives the molecule its color, and since 1870 researchers have studied the structural properties of chemical compounds as well as their colors, as they believed that nitro compounds, quinones and aromatic compounds are very colorful as these colors It may be removed or diminished if the compounds are hydrogenated [24].The phenomenon of unsaturation that gives compounds the ability to absorb hydrogen comes as a result of the presence of electrons between specific pairs of atoms that are not well fixed within covalent bonds, but this does not negate their presence within molecular orbitals, where they may bind to several atoms These electrons, within a certain wavelength

range, can absorb energy from the light, and it is the reflection or transmission of the remaining light that gives the compound its noticeable color [24].

1.4 Types of Organic Dyes

The active medium in laser dyes consists of specific solutions of an organic dye dissolved in a liquid methyl ethyl alcohol, methyl alcohol, or water. Laser dyes have a high absorption capacity in the ultraviolet and visible regions of the spectrum depending on the chemical compositions.[13].

Dyes are classified according to the wavelength of the radiation they emit, where each group emits a specific range of the spectrum ranging between (400-1000 nm) depending on its chemical composition [14]. Laser dyes are classified according to chemical structure into the following [15]:

1. (Polymethine) dyes :It is emitted in the red or near-infrared range (700 -1000) nm .
2. Xanthene dyes (500-700) nm.
3. Coumarin dyes: It is emitted (blue-green) region i.e ,(400-500) nm.
4. (Scintillator) dyes: It is emitted in the ultraviolet region wavelength less than (400) nm.

For effective performance, laser dye molecules should have the following characteristics [1].

1. It has high photochemical stability.
2. It has a high solubility in a large number of solvents without generating molecular complexes and responds to the auxiliary factors used to overcome the formation of these complexes.
3. It should have a wide emission beam, i.e. a wide toning range.
4. The absorption spectrum of the dye must match the spectral distribution of the pumping source.
5. It has a high quantitative output during the dominance of radioactive transitions. Figure (1.3) shows The wavelength range of different dye lasers.

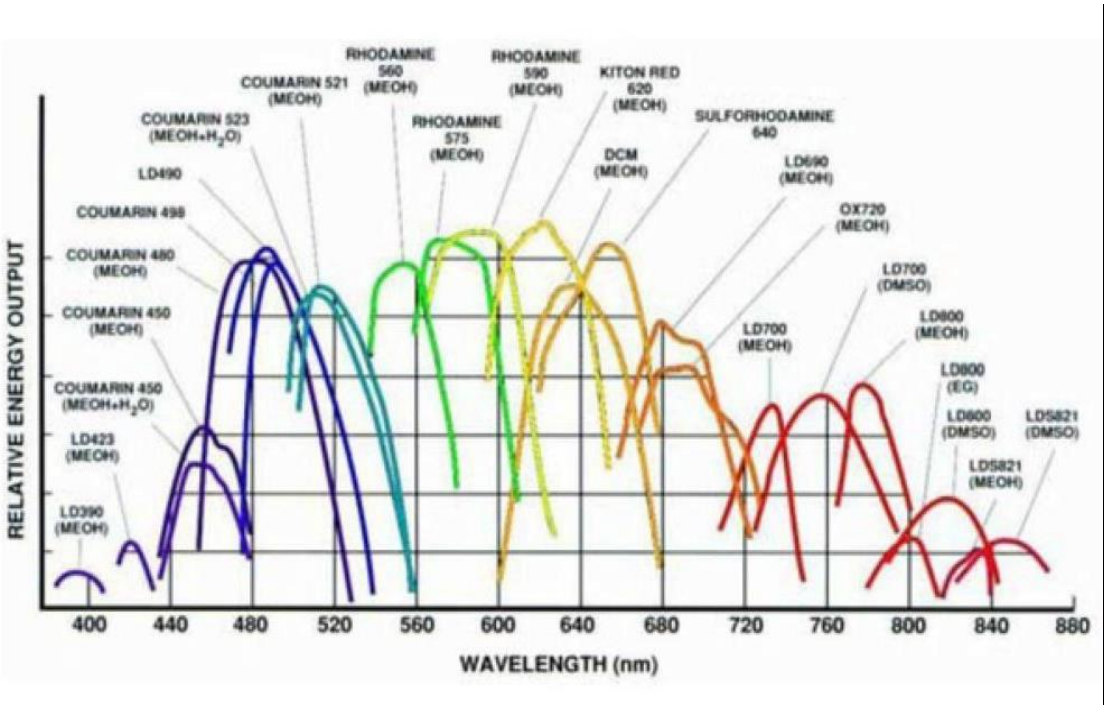

Figure (1.3): The wavelength range of different dye lasers

1.5 Methylene blue dye

Methylene blue is an organic chloride salt with a formula $C_{16}H_{18}ClN_3S$. It is also called Methylthionine chloride or Swiss Blue. It is a thiazine dye with antioxidant, cardioprotective properties, antimalarial, and an antidepressant. It is soluble in glycerol, water, chloroform, glacial acetic acid, and ethanol. It is slightly soluble in pyridine and insoluble in ethyl ether, oleic acid, and Xylene. It is a synthetic basic dye. When its administration route is intravenously and in low doses, it converts methemoglobin to hemoglobin. It functions as a histological dye, tracer, acid-base indicator, neuroprotective agent, fluorochrome, etc. This compound was first synthesized by Heinrich Caro in the year 1876. It is obtained as a dark green crystalline powder or crystal with a bronze-like luster. When dissolved in an alcohol solution or water it gives a deep blue color. It is widely used in treating methemoglobin levels greater than 30%. The figure shows the structure of the methylene blue dye [32,33,34].

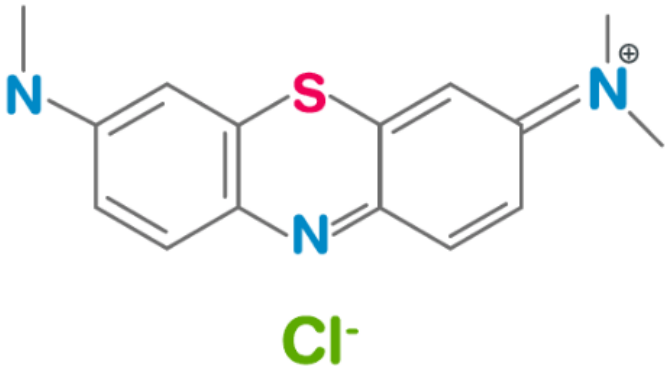

Figure (1-4) Structure of Methylene blue – ($C_{16}H_{18}ClN_3S$) [33].

1.6 SiO_2 Nanoparticales

Silicon dioxide, also known as silica, is an oxide of silicon with the chemical formula SiO_2, most commonly found in nature as quartz and in various living organismsIn many parts of the world, silica is the major constituent of sand. Silica is one of the most complex and most abundant families of materials, existing as a compound of several minerals and as a synthetic product. Notable examples include fused quartz, fumed silica, silica gel, opal and aerogels. It is used in structural materials, microelectronics (as an electrical insulator), and as components in the food and pharmaceutical industriesIn the majority of silicates, the silicon atom shows tetrahedral coordination, with four oxygen atoms surrounding a central Si atom (see 3-D Unit Cell). Thus, SiO_2 forms 3-dimensional network solids in which each silicon atom is covalently bonded in a tetrahedral manner to 4 oxygen atoms. In contrast, CO_2 is a linear molecule. The starkly different structures of the dioxides of carbon and silicon are a manifestation of the double bond rule.

SiO_2 has several dean crystalline forms, but they almost always have the same local structure around Si and O. In α-quartz the Si–O bond length is 161 pm, whereas in α-tridymite it is in the range 154–171 pm. The Si–O–Si angle also varies between a low value of 140° in α-tridymite, up to 180° in β-tridymite. In α-quartz, the Si–O–Si angle is 144°[33].

1.7 Literature Review

Several researches used methylene blue dye for studying nonlinear optical properties

- In **(2003)** R.Ganeev *et al*. [35],they have studied the Z-scan technique at wavelength (1064 nm), the nonlinear refraction, nonlinear absorption, and saturable absorption of polymethine dyes. The coexistence of several nonlinear optical processes in dye solutions driven by picosecond pulses was explored, which found to be quite interesting. A number of different models were used to compute the saturable absorption. On a variety of polymethine dyes, Nonlinear refractive indices, nonlinear absorption coefficients, and saturation intensities were determined utilizing nonlinear refractive indices, nonlinear absorption coefficients, and saturation intensities.
- In **(2008)** H.Tajalli et al., studied the absorption and fluorescence spectra of the high-fluorescent laser dye (Nile Red) and the oxazine cationic dye (Nile blue) in different solvents as a function of the polarity and type of solvent. The interaction of the dye with the anisotropic surroundings and the interaction of isotropic solvents were examined and compared using optical spectroscopy. The spectral shifts were related to the polarity of the solvent and nature. The photoelectric effect of guest-host systems in an electro-optical system was also investigated using the method of polarized spectroscopy, dichromatic ratios, degree of anisotropy, and the dichromatic ratios of these dyes were investigated in liquid crystal hosts[36].
- In **(2009)** Q. Mohammed [37], they have studied nonlinear optical and optical limiting properties of Chicago sky blue 6B doped PVA film at (633 nm) and (532 nm) studied using a continuous wave laser. The sign and magnitude of the third-order nonlinearity from the closed aperture Z-scan data while the nonlinear absorption properties were assessed using the open

aperture data. The Chicago sky blue 6B doped PVA film exhibited nonlinear saturated absorption and strong self-defocusing effect. The limiting effect of the sample was studied and the results indicate that the film possesses good characteristic of optical limiting.

- In **(2012)**, R**.**Manshad and A. Hassa, [38], they have Studied the single beam Z-scan technique was used to determine the nonlinear optical properties of the orcein dye in the solvent chloroform and a dye doped polymer film. The experiments were performed using CW solid state diode laser with a wavelength of (532 nm). This material exhibits negative optical nonlinearity. Optical limiting characteristics of the dye solution and polymer film were studied. The result reveals that orcein dye can be a promising material for optical limiting applications.
- In (**2012**) H. O. Seo *et al* [39, they have this research was studied by preparing very thin films of Tio2 and covered with a very thin shot of SiO2 and a thin layer of methylene blue was adsorbed in aqueous solutions. The absorption capacity was studied in ml of both cases, and the results showed high absorption capacities. This high adsorption capacity is similar to methylene blue in TiO_2 samples covered with, sio2.After discussing the high adsorption capacity, a simple re-plasticization was done to Thermal decomposition of methylene can be facilitated, the MB adsorption capacity of TiO2/SiO2 was fully recovered.
- In (**2018**) M Rao *et al*. [40]. The researchers, based on the z-scan technology supported by a femto and Pico nanosecond laser, measured the nonlinear properties of glass slides containing bismuth and barium. The linear properties of glass were studied with UV-visible absorption studies. This study reveals that the content of bismuth in the glass mesh leads to an increase in the absorption in the glass. Three-photon absorption (3PA) and free carrier absorption (FCA) are prevalent in BBB glasses. The optical

absorption and trans-absorption properties of BBB glasses have also been reported.

- In (**2019**) N. Shokoufi *et al*.[41] , studied the nonlinear properties of dye (methylene blue (MB)) and plasmonic nanoparticles (gold nanoparticles (GNPs)). This study relied on Z-scanning with continuous wave (CW) pumped solid state lasers (DPSSL). Nonlinear parameters (NLR (N2) and NLA) ((were determined β)) were determined. Scientologists have attributed the nonlinear refraction and the and nonlinear thermal effects. Z-scan show a significant increase in the nonlinear parameter.
- In (**2020**) S. Wang *et al*[.42], they have studied the nonlinear optical properties of rubidium vapor using z-scan technique in order to improve and improve the nonlinear optical processes. And finding nonlinear optical applications in quantum optics. These properties were also explained under different experimental conditions. Where the nonlinear Kerr refractive index n_2 was obtained from the measured dispersion curve, and it mainly occurs in the range of 10^{-6} cm^2/W. The direct measurement of the nonlinear Kerr coefficient was also used in understanding nonlinear optical processes

- In (**2021**) A. Awalludin *et al*. [43] used the z-scan technique to study the nonlinear optical properties of the fuchsin dye solution, where the nonlinear refraction (NLR) and nonlinear absorption (NLA) of the fuchsin dye solution were measured. Four different concentrations of dye were taken (0.03 mm, 0.05 mm, 0.10 mm, and 0.20 mm). The results of this study showed a decrease in the value of the NLR and the value of the NLA increased with the increase in the concentration. This study showed that acid fuchsian dye has an optical limiting ability due to the appearance of NLR and NLA reducing properties at 0.05 mM. And it showed that the low

optical limit (OL) is about 0.04 W under the continuous laser beam (CW) 532 nm.

In (**2022**) O. Ovchinnikov *et al*. [44], they have studied methylene blue in order to improve the properties of nonlinear absorption through core/shell Au/SiO2 nanoparticles. The researchers analyzed in this study the nonlinear optical properties of the thiazine contribution dye molecules of methylene blue (MB+), located in the near-field region of spherical gold nanoparticles, coated with a shell of silicon dioxide (Au/SiO2 NPs). The results of the study showed that the saturated reverse absorption characteristic of MB + dye was increased in the presence of gold nanoparticles using Z-scanning technology. The study concluded that the increase in the effective triple adsorption cross-section of MB + particles in the presence of Au/SiO_2 NPs makes the observed effect larger.

1.8 The aim of the work

Preparation(MBD/Sio2) nanoparticles film and study the linear and nonlinear properties of methylene blue dye doped with (SiO_2) nanoparticles at different weights (0, 0.01, 0.03 and 0.05 gm), by Z-scan technique .

2.1 Introduction

This chapter is the theoretical part of the study, we will have a general description of the theoretical part which will be interpreted with our results of, this chapter include physical concepts, relationships, scientific clarifications, and laws used.

2.2 The Optical Properties :

The optical properties give us an explaining about the interaction between the light and materials. The optical properties of materials are those that are revealed when the material interacts with electromagnetic radiation. These properties explain different phenomena such as color, transparency, or opacity. At the molecular level, different structures of materials cause light to be absorbed and reflected in different ways, producing diverse effects. Understanding these phenomena is essential in many current technologies, such as those based on optical fibers [48-50]. These metal oxides have the characteristic of a rapid increase in absorption when the energy of the absorbed radiation is equal to the energy of the prohibited field, which separates the two bands of equivalence and conductivity and is called the basic absorption edge. the following

$$R + T + A = 1 \ldots\ldots\ldots\ldots (2\text{-}1)$$

Where: R-reflectivity, T- transmittance, A-absorbance

2.2.1 Linear optical properties

The interaction between the nature and distribution of charges inside the material (electronic, molecular ,or ionic) and electromagnetic radiation leads to the appearance of the optical properties of materials [52].

When the electromagnetic radiation falls on the material and interacts with it, many processes occur as part of the electromagnetic radiation is absorbed by

the material and the other part is called the transmitting ray because it passes through the material while another part of the electromagnetic radiation is reflected from the surface of the material called the reflected part [53].

In order to obtain information about the interference composition of the material and the nature of its bonds it is necessary to know the transmittance, absorption and reflectivity of the electromagnetic radiation falling on the material For example the energy packets and the quality of transitions within the material are identified by studying the ultraviolet spectrum but to know the field of practical applications in which materials are used the visible spectrum must be studied [54].

2.2.2 Absorbance

When light falls on a medium, part of the light is transmitted through the medium, part is reflected, and part is absorbed through the medium. The term absorbance is used a lot in analytical chemistry. When we use the expression absorption usually, we refer to the physical process of absorbing light, while when we talk about the mathematical quantity, we use the expression absorbance.

While dispersion refers to, the scattered incident light by the suspended particles, and will not actually be absorbed. In this case, the term "attendance" is preferred, which explains the losses due to scattering and scintillation [51,52].

$$A = \log\frac{I_0}{I} \ldots\ldots\ldots\ldots (2.5)$$

Where:

I: Is the radiant flux in the material.

I_0 : Is the incoming radiant flux.

2.2.3 Transmittance

The part of the light that is not absorbed and goes out of the material is called transmittance.

When the medium is completely transparent, all light is transmitted without absorption.

The optical transmittance is given by law [53,54]

$$T_\lambda = \frac{I}{I_0} \dots\dots\dots\dots (2.6)$$

The absorbance is related to the optical transmittance:

$$A_\lambda = -logT_\lambda \dots\dots\dots\dots (2.7)$$

$$I = I_0 . e^{-\alpha . t} \dots\dots\dots\dots (2.8)$$

α: the linear attenuation coefficient.

2.2.4 Absorption Coefficient (α)

The absorption coefficient (α) indicates that incoming light ray is subjected gradual decrease in its energy flow.

The absorption coefficient (α) expresses this reduction over a unit area along the direction of wave diffusion inside a medium. Therefore, the absorption is related to the energy of the incoming radiation and the energy gap of the material which receives the radiation.

properties of the semiconductor regarding the gap energy of the semiconductor and the type of electronic transitions.

the equation (2.7) of absorption of ray:

Where: (t) is the distance which radiation move in the matter (α) refers to the absorption coefficient, it's usually measured by cm^{-1}.

The absorption coefficient can be written with the form [55]:

$\alpha = \frac{1}{d} 2.303 \log(\frac{1}{T})$…… (2.9)

where T: Transmittance, d: thickness

2.2.5 Extinction Coefficient (k_o)

As we know the refractive index written by the imaginary part and rea part in a complex from.

The imagery part refers to the extinction Coefficient

The general relationship of refractive index [56]: n : complex part.

$n = n_0 - iK_0$ ……. (2.10) n: the real part.

Generally, the complex part in the refractive index depends crystal structure, crystal defects and refers to the extinction coefficient.

This part given [57] in:

$k_0 = \frac{\alpha\lambda}{4\pi}$ …… (2.11)

Where λ: is the wavelength of incident photon rays.

2.2.6 Refractive index

The absorption coefficient expresses the interaction of the particles of the material with the electromagnetic waves falling on them.

The refractive index is the ratio of the velocity of a light wave in a vacuum to the velocity of this wave in a medium.

Gives by relationship [58]:

$n = \frac{C}{v}$ …… (2.12)

where C: velocity of a light in the vacuum. v: velocity of a light in the matter.

The refractive index does not have a unit.

When the density of the material increases, the velocity of light propagation through it decreases, and thus the refractive index is greater.

The refractive index is described as a complex number consisting of a real part that expresses refraction and an imaginary part that expresses attenuation.

2.2.7 Dielectric constant

Usually when we study the optical properties, we also study the dielectric. Dielectric constant expresses the ability of a substance to focus electric field lines.

This relates to different frequencies.

At optical frequencies, the electronic polarity is above the remaining types of polarization [59].

We can calculate the real and imaginary dielectric constant from the equation [53]:

$$\varepsilon = \varepsilon_1 - i\varepsilon_2 \dots\dots\dots\dots (2.13)$$

where: ε is the complex dielectric constant and (ε_1, $i\varepsilon_2$) are the real and the imaginary parts of the dielectric constant, respectively, which are related to n and K_o values as shown in the following equations [53]:

$$\varepsilon = n^{*2} \dots\dots\dots (2.14)$$

$$(n - ik_0)^2 = \varepsilon_1 - i\varepsilon_2 \dots\dots\dots.. (2.15)$$

Then the real and imaginary complex dielectric coefficient can be written as follows:

$$\varepsilon_1 = \left(n^2 - {k_0}^2\right) \dots\dots\dots (2.16)$$

$\varepsilon_2 = (2nk_0) \ldots\ldots\ldots (2.17)$

The optical conductivity (σ_{op}) depends directly on the refractive index (n), (c) is speed of light and absorption coefficient (α) by the following relation [53]:

$$\sigma_{op} = \frac{\alpha nc}{4\pi} \ldots\ldots\ldots\ldots (2.18)$$

2.3 Absorption Regions:

Absorption is divided into three regions as in figure (2-1):

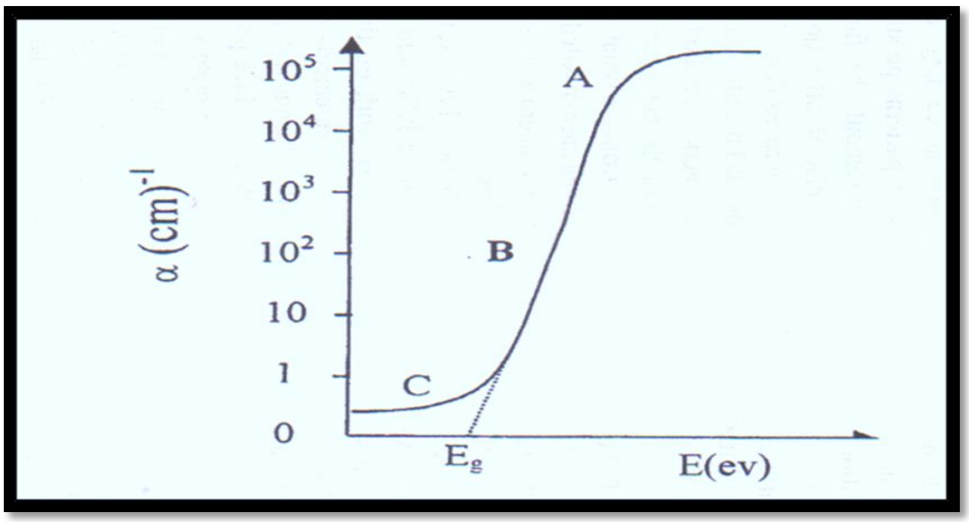

Figure (2-1): The variation of absorption edge with absorption regions [60]

A. High Absorption Region

We can see this absorption in part (A) in the Figure (2-1), when (α) is greater than 10^4 cm^{-1}.

B. Exponential Region

When the value of the absorption coefficient (α) is (1 cm $^{-1} < \alpha < 10^4$ cm $^{-1}$) as we see in part b of the figure (2.1)

With this value of absorption coefficient, the transition between the levels extending from the Valens band to the local level in the conductive band and

vice versa, the transition from the levels local in Valens band to extended levels in the lower part of the conductive band. Extending from the Valens band to the local level in the conductive band and vice versa, the transition from the levels local in (Valence to extended levels in the lower part of the conductive band [60].

C. Low Absorption Region

In part (c) in Fig. (2.1) in this region the absorption coefficient it is approximately ($\alpha < 1 cm^{-1}$). The state density is large within the space motion resulting from structural errors and in this case, transitions occur in this region [61].

2.4 The Electronic Transitions

There are two types of the electronic transition:

1- Direct Transition

In this type: because of the bottom of (Conductive) is exactly over the top of (valence Band.) the wave vector before transition equals the wave vector after the transition. So that r. ($\Delta K=0$).

The absorption appears when the direct transitions are in two types [62]:

$$\left(h\nu = E_g{}^{opt}\right) \dots\dots\dots\dots (2.19)$$

a. **Direct Allowed Transition**:
When the top of the valence) and the bottom of the conductivity band. as shown in figure (2-2).

- **Direct Forbidden Transitions:**

In this case the electron transport directly from the top of valance band with is near the bottom of conductor band. We can see this in figure The absorption coefficient equation in this case will be with the form [63]:

$$\alpha h\nu = B(h\nu - {E_g}^{opt})^r \dots\dots\dots (2.20)$$

Where:

E_g^{opt}: A direct transition energy gap

B: is the constant of material type

r: exponential constant, its 1/2 in the allowed direct transition and 3/2 in the forbidden direct transition.

- **Indirect Transitions:**

Indirect transformations occur when, in the curve (E-K), the bottom of the symmetry band is not above the top of the conductor band.

In this case, a valence electron moves in a non-perpendicular way to the conductivity, so the value of the wave vector of the electron is not the same in after and before transition.

This phonon process is carried out in order to achieve the conservation of energy and momentum.

The indirect transmission in two types [63]:

- **Allowed Indirect Transitions:**

The permissible indirect transitions occur between the bottom of the conductivity band and the top of the valence band in the K-space region, as shown clearly in Figure (2.2).

- **Forbidden Indirect Transitions:**

Forbidden indirect transformations occur at the bottom of the conductivity band and above the valence band [64] as in figure (2-2) In this case.

$$\alpha h\nu = B(h\nu - {E_g}^{opt} \pm E_{ph})^r \dots\dots\dots (2.21)$$

(r = 2) indirect transition and (r = 3) forbidden indirect transition.

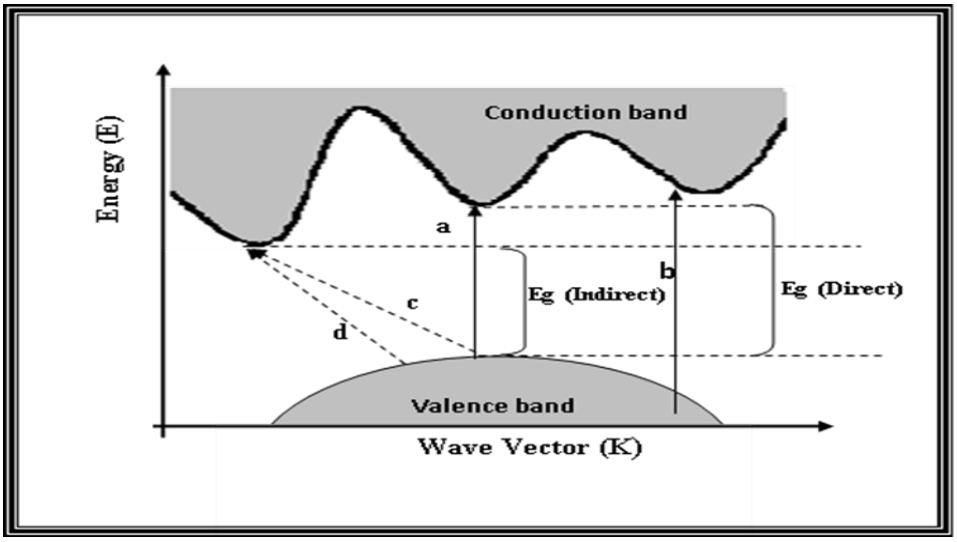

Figure (2-2): The transition types [65,66].

a. allowed direct transition

b. forbidden direct transition d. forbidden indirect transition

c. allowed indirect transition

2.5 Nonlinear Optical Properties

The study of events that develop as a result of changes in the optical properties of materials as a result of intense light contact is known as nonlinear optics.

Nonlinear phenomena have received a lot of attention [67]. Positively charged particles travel in the direction of applied electric fields, while negatively charged particles go in the opposite direction. The displacement between positive and negative charged particles produces dipole moments, and the dipole moment per unit volume describes the induced polarization of the medium. Electric polarization is approximately linearly proportional to the applied electric field (E) when the applied electric fields are sufficiently minimal [68].

$$P = \chi . E \ldots\ldots\ldots (2.2)$$

Where (χ) is the electric susceptibility tensor. In the case of linear optics, this is the case. When the applied electric fields are high enough, however, the induced polarization has a nonlinear dependence on them and may be described as a power series with respect to them:[69]

$$P = \chi^{(1)}.E + \chi^{(2)}.EE + \chi^{(3)}.EEE + \cdots \quad \ldots\ldots\ldots (2.3)$$

$$P = P^{(1)} + P^{(2)} + P^{(3)} + \cdots \quad \ldots\ldots\ldots.. (2.4)$$

Where $\chi^{(1)}$ is the linear susceptibility, $\chi^{(2)}$ is the second order nonlinear susceptibility, and $\chi^{(3)}$ is the third order nonlinear susceptibility The term $\chi^{(1)}$ is responsible for linear absorption and refraction, and is the only term that reflects the linearity between the induced polarization and the incident electric field. The term $\chi^{(2)}$ is present only in non-centrosymmetric materials, i.e., materials that do not have inversion symmetry. The third order nonlinear optical interactions, which are described by the term $\chi^{(3)}$ [69]. The field of nonlinear optics (NLO) has been developing for a few decades as a promising field with important applications in the domain of photo electronics and photonics. Organic materials are considered as one of the important classes of third order NLO materials because they exhibit large and fast nonlinearities [70].

2.6 Saturable Light Absorption

A nonlinear process that can be associated with real (rather than virtual) energy levels and population changes in those levels is that of saturable absorption. This process occurred when the nonlinear absorption coefficient (β < 0), which can be appeared when a strong light absorption between two levels causes saturation (bleaching) of the corresponding electronic transition. The two levels involved surface resonance ground and excited state. On the other hand, this is a process in which a material can be highly absorbing at a specific

wavelength when a low-intensity beam is incident upon the material, yet an

extremely intense beam (at that same wavelength) will pass through the medium with little change in intensity [77].

2.7 Two Photon Absorption (TPA)

Two-photon absorption is defined as the simultaneous absorption of two photons of the same or different frequency in order to excite a molecule from one state (usually the ground state) to a higher energy electronic state (TPA). The process of two-photon absorption occurs when the energy difference between the implicated lower and upper states of the molecule is equal to the total of the energies of the two photons, as in the case of a saturable absorber. This process occurred when the nonlinear absorption coefficient ($\beta > 0$). This effect is shown in Figure (2.8). The two-photon transition rate can be significantly enhanced if an intermediate level (3) is located near the virtual level shown by the dashed line in Figure (2.9) [78].

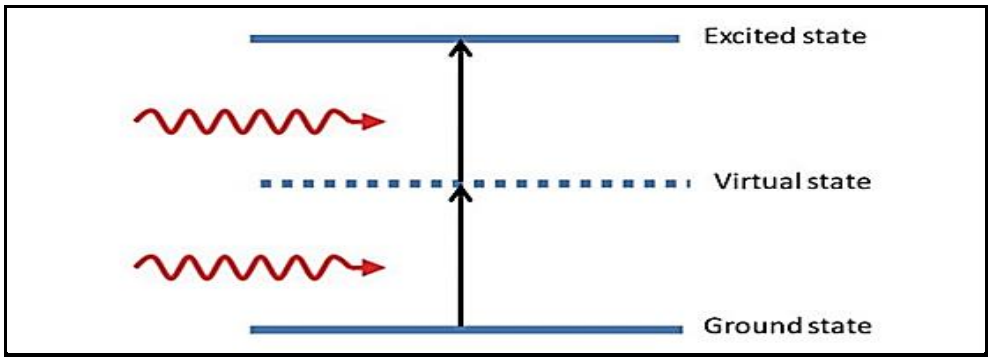

Figure (2.3): Energy levels for two-photon absorption process [78].

2.8 Kerr Effect

The nonlinear electronic polarization, which can be defined as altering the refractive index, is a nonlinear interaction of light in a material. The Kerr effect can produce a local change in the refractive index in high-intensity laser beams, causing the laser material to operate as a lens. This can cause laser beams to self-focus [79].

2.9 Z-scan technique

Z-scan technique for studying the photophysical properties of materials. This technique depends on focusing laser beams in the z direction to the sample plane. This transmitted signal has two possibilities, the first is to go directly to the detector and the second is to go through an opening to the detector. Then a function is graphed between the magnitude of the detected signal and the position of the sample[70].

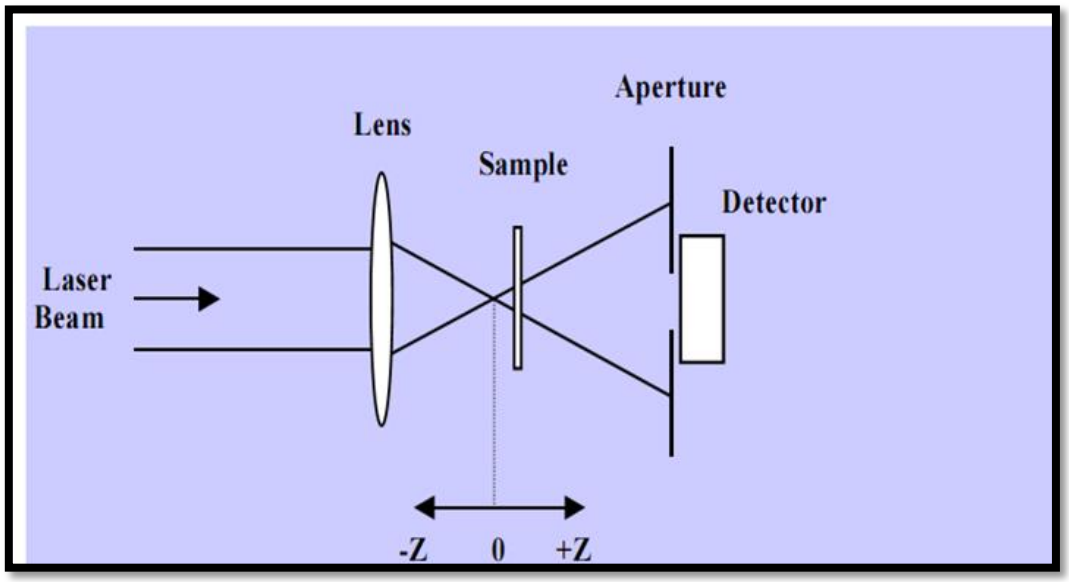

Figure (2-4: Illustration of the experimental setup for z-scan [70].

When studying the sample of the material under investigation through the focus of the laser beam, then measuring the radius of the beam (or intensity of the axis) at a point behind the focus as a function of the position of the sample. These quantities are affected by the autofocus effect

Figure (2-4) Aperture transmission measurement as a function of sample position. The left detector is used to monitor the energy of the incident pulse.

We observe the nonlinear absorption, by measuring the absorption of each photon separately. By recording the strength of the entire transmitted beam. Using this data, the measurement of nonlinearity can be corrected.

Z-scan technology is used to measure the nonlinear refractive index n and measure the refraction and nonlinear absorption in the material, which can simultaneously measure the nonlinear absorption bracelet in liquids, solutions, gases, solids and non-linear refraction in solids, liquids and liquid solutions. And that through the application of a single laser beam. Therefore, this method is often used because it is easy, accurate and quick to implement, and There are two use cases for the system (Z-Scan).

2.9.1 Z-Scan closed an aperture

In a closed-aperture Z-scan the nonlinear refractive index n_2 can be calculated from the following formula [2.21]. If a material with a negative nonlinear refraction index and a thickness lower than the diffraction length of the focused beam is utilized, the Z-Scan transmittance as a function of Z is related to the sample's nonlinear refraction. This can be thought of as a narrow variable focal length lens. The beam irradiance is modest and nonlinear refraction is minimal distant from the focus (Z_0).

The measured transmittance remains constant in this situation (i.e., Z-independent). Irradiance increases as the sample approaches the beam focus, causing self-lensing in the sample [71].A negative self-lens in front of the focal plane will tend to collimate the beam aperture in the far field, increasing the iris position transmittance.

Following the focal plane, the same self-defocusing increases the beam divergence, causing the beam to diverge at the aperture and lowering the measured transmittance. Far from focus (Z >0), nonlinear refraction is modest,

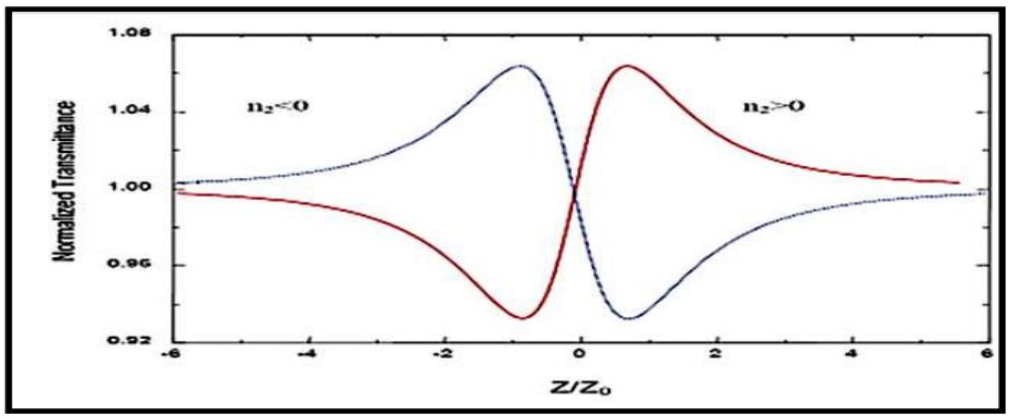

Figure (2.5): **Calculated Z-Scan transmittance curves for a cubic nonlinearity [72].**

$$n_2 = \frac{\Delta\Phi_0}{I_0\, l_{eff}\, k} \dots\dots\dots (2.22)$$

where:

$$k = \frac{2\pi}{\lambda} \dots\dots\dots (2.23)$$

$\Delta\Phi_0$**:** nonlinear phase shift.

λ: is the wavelength of the beam.

I_0**:** is the intensity at the focal spot.

l_{eff}**:** is the effective length of the sample which can be determined from the following formula [71]:

$$l_{eff} = \frac{1 - e^{-\alpha_0 L}}{\alpha_0} \dots\dots\dots\dots (2.24)$$

Where:

L: the sample length.

α_0**:** linear absorption coefficient.

The intensity at the focal spot is given by [71]:

$$I_0 = \frac{2P_{peak}}{\pi\omega_0} \ldots\ldots\ldots\ldots (2.25)$$

Where:

ω_0**:** the beam radius at the focal point.

P_{peak}**:** the peak power given by

$$P_{peak} = \frac{E}{\Delta t} \ldots\ldots\ldots (2.26)$$

Where:

E: the energy of the pulse.

Δt: the pulse duration.

The closed-aperture Z-scan defines variable transmittance values, which used to determine the nonlinear phase shift $\Delta\Phi_0$ and the nonlinear refractive index n_2 using the above equations

2.9.2 Z-Scan open aperture

Open aperture Z –scan was used to in investigate the nonlinear absorption coefficient by removing the aperture. This case corresponds to collecting all the transmitted light and therefore it is insensitive to any nonlinear beam distortion due to nonlinear refraction [71,72].

The coefficients of nonlinear absorption can be easily calculated from such transmittance curves. The total transmittance is given by [71]:

$$T(Z) = \sum_{m=0}^{\infty} \frac{\left[\frac{\beta I_0 L_{eff}}{1 + (Z/Z_0)^2}\right]^m}{(m+1)^{3/2}} \ldots\ldots\ldots (2.27)$$

Where:

Z: is the sample position at the minimum transmittance.

Z_0**:** the diffraction length.

m: integer

T(z): the minimum transmittance.

Z-Scan with a fully open aperture is clearly insensitive to nonlinear refraction, even with nonlinear absorption (thin sample approximation). With no aperture, the Z-Scan traces should be symmetric with regard to the focus (Z = 0), where they should have the lowest transmittance (e.g., multiphoton absorption) or maximum transmittance (e.g., saturation of absorption). In fact, the coefficients of nonlinear absorption can be easily calculated from such transmittance curves. Nonlinear absorption coefficient (β), can be easily calculated by using the following equation:[73]

$$\beta = \frac{2\sqrt{2}T(z)}{I_0 l_{eff}} \ldots\ldots\ldots (2.28)$$

Where T(z): the minimum value of normalized transmittance at the focal point, (Z=0). It should be clear that the transmittance versus sample position graph of such an open aperture Z-Scan should be symmetric around the focus as shown in Figure (2.5).

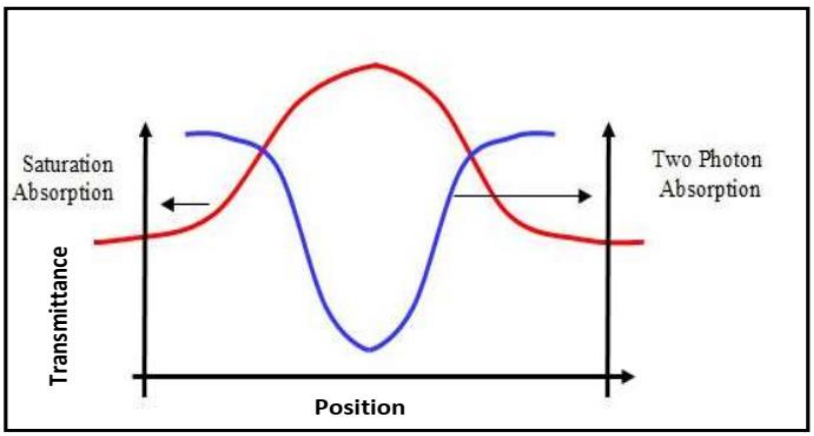

Figure (2-6): Open aperture Z-Scan curve [73]

3.1 Introduction

This chapter includes the materials used in the work and their method of preparation, as well as some devices used in the characterization of the prepared samples, such as the optical microscope, , spectrophotometer, and the Z-scanning technique.

3.2 The Utilized Materials

The following materials were used in this study:

- **Methylene Blue Dye (MBD)**

Methyl blue (MB) is a soluble dye in a different sol-vent, which is widely used in the in-research laboratories. MB was chosen as the model dye in this research. The methylene blue dye has the physical properties shown in the table (3-1) [34].

Table (3-1): The physical Properties of Methylene blue dye [34].

Methylene blue	**$C_{16}H_{18}ClN_3S$**
Molecular Weight of Methylene blue	319.85 g/mol
Trade names	Urelene blue, Prove blue, Provable
Melting Point of Methylene blue	100 to 110 °C
Routes of administration	Mouth and IV

- **Silicon Oxide (SiO_2) Nanoparticles**

We will add silicon dioxide nanoparticles in the form of white powder with a size of (Size: 20-30 nm, purity: 99.8%). from company (Hongwa Inter National Group Ltd.-China).

3.3 Preparation of Nanocomposites Films

Film samples were prepared consisting of (MB/SiO_2) Nanocomposite films samples were prepared according to the following steps:

I- Nanocomposites films were prepared by pouring 100 ml of chloroform alcohol into a 100 ml volumetric flask, adding 0.2 gm of methylene blue dye with different concentrations which are (0.01, 0.03 and 0.05) gm. of nanoparticles SiO_2. The flask is placed in a magnetic rotating device with a frequency of 1.2 kHz, then the agitator is placed inside the flask to stir the alcohol until complete dissolution for 30 minutes at a temperature of 150 ° C to obtain a more homogeneous solution and then wait until the solution cools.

Figure (3-1): image (drip and wipe method).

II- The same steps 1 and 2 are repeated with the addition of of nanoparticles until complete dissolution and then drop it on a glass slide.

III- The same steps are repeated 1, 2 and 3 with a change in the weight ratios of the nanoparticles to obtain other dyes.

IV- The samples thickness was measured, it is found to be in the range of (15- 25) µm. The stages of the experimental work and procedure are illustrated in Figure (3-2).

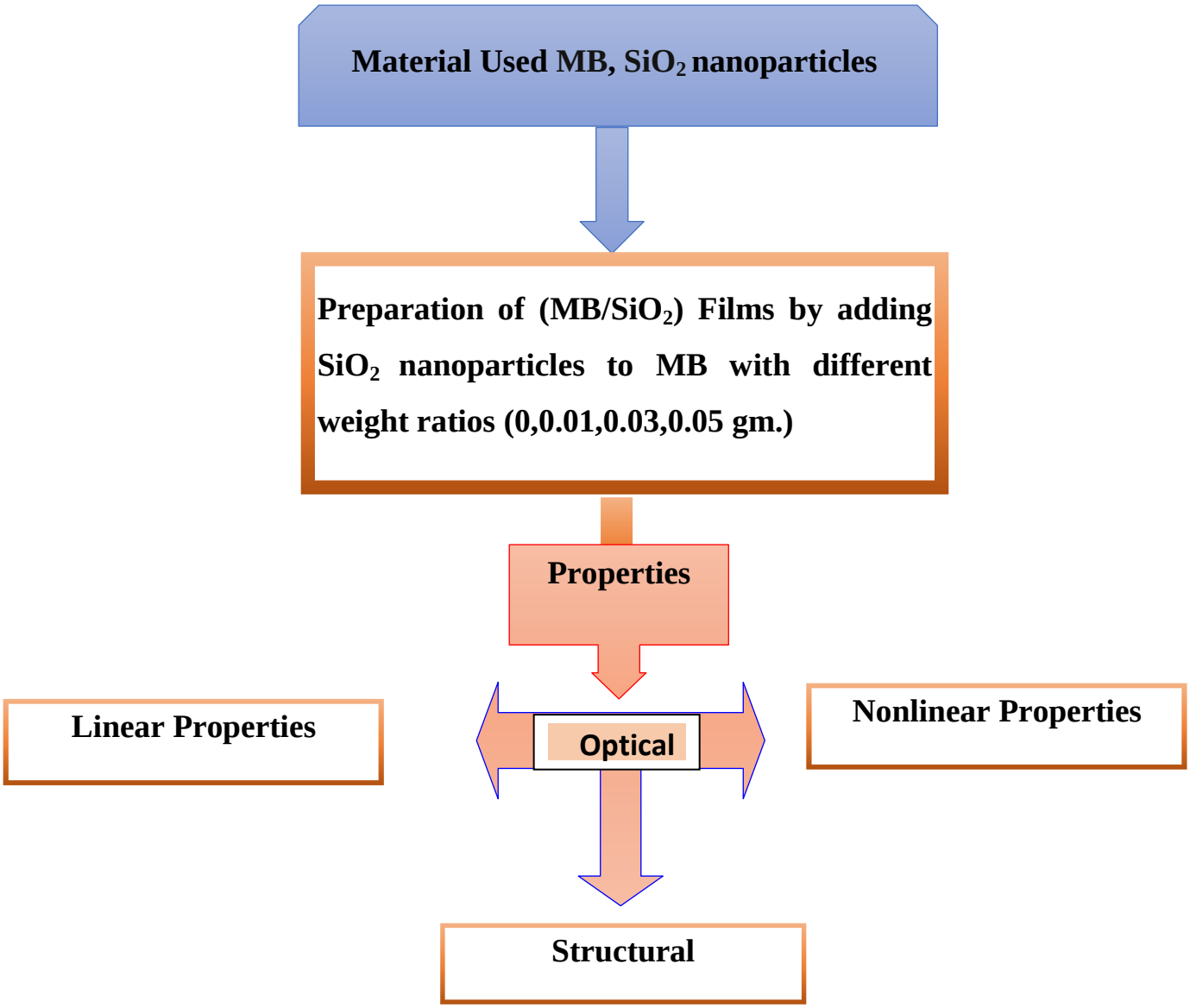

Figure (3-2): The Scheme of (MB/SiO_2 nano) films and the structural, optical and Nonlinear properties.

3.4 Measurements of Structural Properties:

3.4.1Optical Microscope

The as-prepared nano-sample (MB/SiO_2) was structurally examined using an Olympus Toup View optical microscope (Nikon-73346) equipped with an automatic light intensity control camera. It has a magnification power (10x and 40x) and this device is located in University of Babylon / College of Education

for Pure Sciences, Department of Physics, which is shown in the the following figure (3.3).

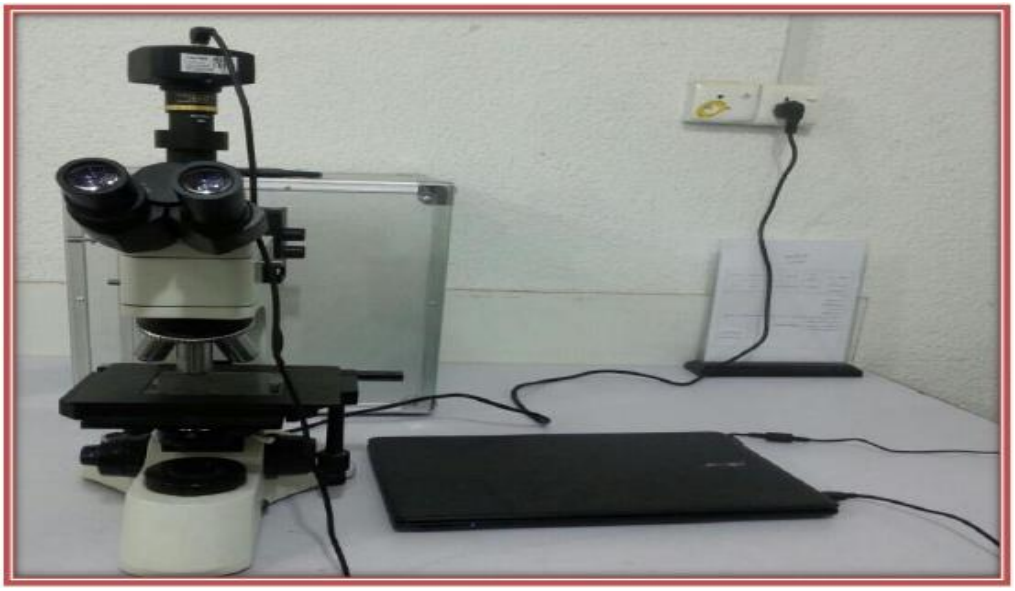

Figure (3.3): optical microscope

3.4.2 UV-VI Spectrophotometer

The fields of spectroscopy are generally distinguished according to the wavelength range in which the measurements are made, and among these areas we can distinguish: ultraviolet, visible and infrared rays, and in this technique we will measure spectrophotometry in the ultraviolet and visible fields, It is a technique for determining optical properties, and the principle of this technique depends on the interaction of light with the sample to be analyzed, and part of the incident beam is absorbed or passed through the sample, when the material absorbs light in the ultraviolet and visible range, the absorbed energy causes disturbances in the electronic structure of the thin films This results in a transfer of electrons from a lower energy level to a higher energy level [74].

For this purpose, we used (Shimadzu, UV-1800 OA, JAPAN) AS Shown in Figure (3.5). The Absorption Spectrum is Recorded at room temperature.

Figure (3-4): UV photographic of spectrophotometer

3.4.3 Z-Scan System

The nonlinear optical properties for (MB/SiO_2) nanocomposites films are explained through Z-scan measurements to determine the nonlinear refraction index and the nonlinear absorption coefficient. In this work, used CW diode laser was used to measure of NLO properties of (MB/SiO_2) nanocomposites films by Z-scan technique. *Z*-scan experiments were performed using 532 nm (CW) solid state laser, (maximum power is 50 mW, which was focused by 15 cm focal length lens. The laser beam waist ω_o at the focus is measured to be 0.4 cm and detector. The sample put in quartz cell was scanned using transition system along direction Z-axes through the focusing area. Z- Scan experiment illustrates in the Figure (3.5). This work was prepared in (College of Education / University of Babylon).

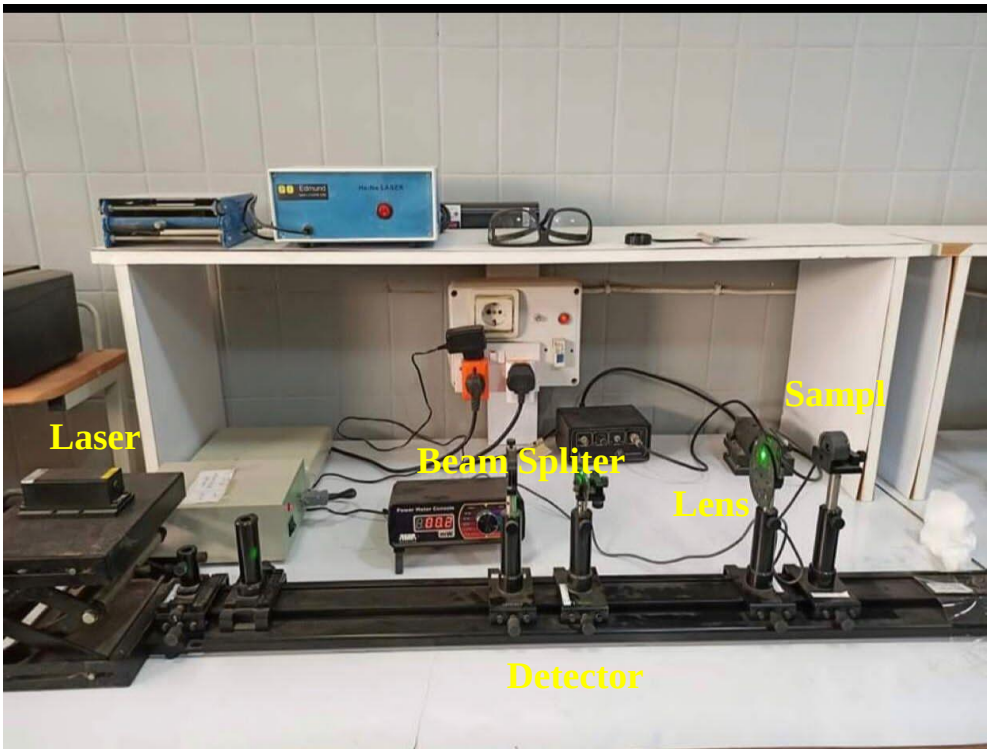

Figure (3-5): Schematic diagram of Z- Scan Technique

4.1 Introduction

In this final chapter which includes the discussion and results of the prepared samples (Methylene Blue Dye/ SiO_2). The results of the characterization of these nonlinear structural and optical films were analyzed using optical microscopy and spectrophotometer, by which the absorption and transmittance were obtained, and then the absorption coefficient and the attended field were calculated through some relations. The dielectric constants, damping coefficient and refractive index were also compared. The reason for changing these characteristics.

4.2 The Structural Properties

The structural properties of methyl blue dye added to it silicon oxide was studied using a microscope.

4.2.1 The Optical Microscope

Show a difference in the surface prepared samples using light microscopy. Photographs of these samples were taken at a magnification (10x and 40x). Figure (4.1) shows optical microscopy images of dopant samples with different concentrations by weight of nanoscale silicon oxide compared to the pure sample. A clear difference was found between the pure and similar sample with increasing concentrations of silicon oxide, as it was found that the increase in the doping concentration with silicon oxide leads to the formation of a continuous network by the filler materials inside the compound, methyl blue dye, which in turn forms paths for charge carriers within these compounds that allow the passage of charge carriers inside the compound. these paths [75]. This results agreement with the results of the previous researcher [76].

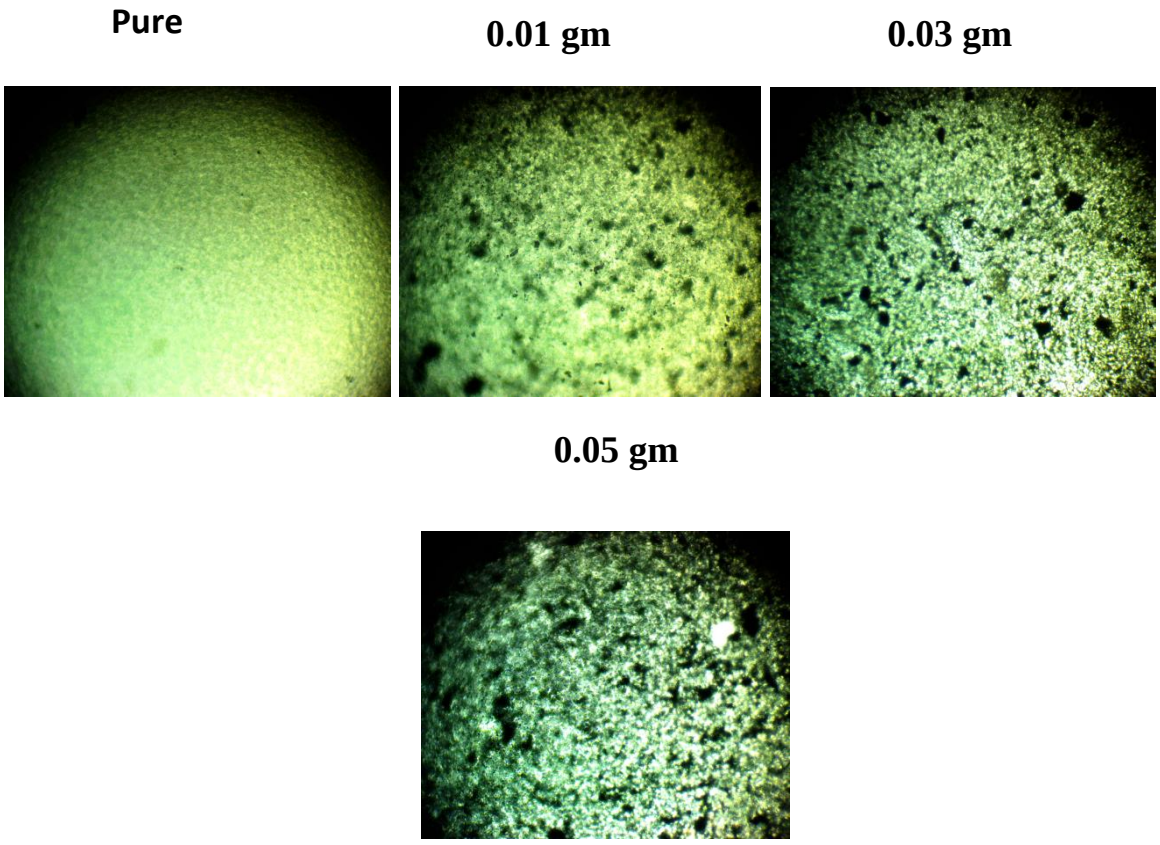

Figure (4-1): morphology (a-10x and b-40x) for (MBD:SiO2) nanocomposites films.

4.3 The Optical Properties

A study of optical properties using spectrophotometry of prepared samples (MBD/SiO_2) aims to know the effect of doping of nano silicon oxide on the methyl blue dye. The absorption and transmittance spectra of samples are recorded using by spectrophotometer, and then the rest of the optical properties are calculated, such as absorption coefficient and optical gap calculation, and damping, refraction, optical conductivity and dielectric constant.

4.3.1 Absorbance (A)

In Figure (4.2), we notice that the change in the absorption spectra relates to wavelength of the incident ray (MBD/SiO_2) nanocomposites films. The absorption of (MBD/SiO_2) nanocomposites with different doping concentrations of silicon oxide was recorded within the spectrum range (400-800 nm). The intensity of adsorption always increases by the increasing addition SiO_2 nanoparticles in the prepared films. That is, there is no chemical reaction between the components of the thin film [77].

It is evident from these absorption spectra that the optical transmittance is reversed, as the absorption spectrum of a pure sample is the lowest possible, then the absorption increases as the doped ratios increase. Similarly, we find that the absorption spectra at the doped ratios 0.03 and 0.05 are the highest possible and almost similar in these two ratios and the highest absorption peak is at ~600 nm wavelength. As for the dopant ratio 0.05, the absorption is highest at 400 nm, then gradually decreases to 800 We find that the absorption spectrum slightly increases from 400 to 650 nm and then starts to decrease to 800 nm. This loss (light wave extinction), which may be caused by several factors in the absorption and scattering caused by the residues of non-reactive molecules [78,79].

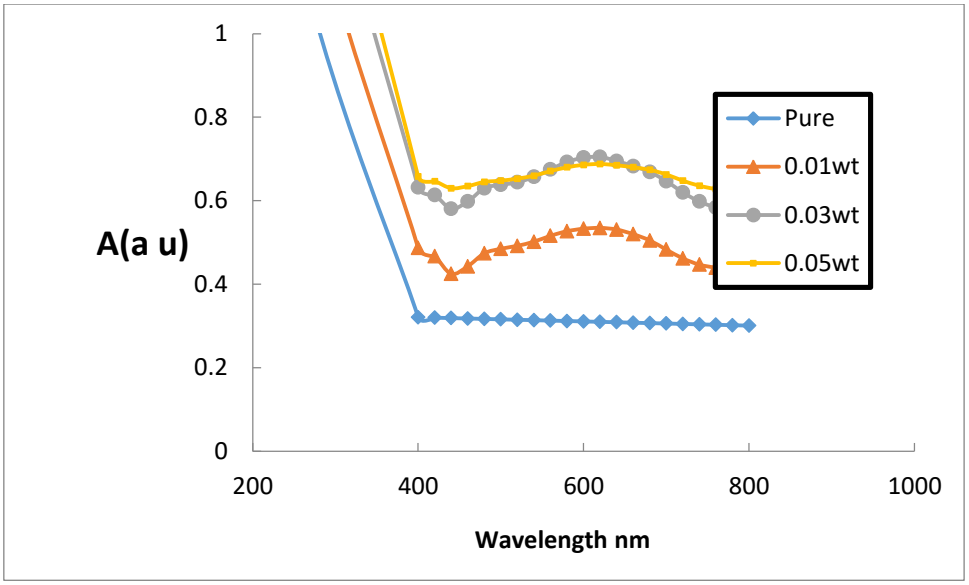

Figure (4.2): The absorbance spectra as function of wavelength λ(nm) of (MBD/ SiO_2) nanocomposite film at deffent value of Sio_2

4.3.2 Transmittance (T)

Optical transmittance was calculated and illustrated in Fig. (4-3) The transmittance (T) as a function of wavelength of (MBD/ SiO_2) nanocomposites. The figure (4.3) shows that permeability for all samples decreases by increasing concentration of nanoparticles (SiO_2), and, this is in agreement with [80].

The change and decrease in the optical transmittance of the prepared samples was observed with increase in percentage doping of silicon oxide. The explanation for this is the presence of free electrons in the outer orbitals of SiO_2 nanoparticles and the transfer of electrons to higher energy levels. As a result of their absorption of magnetic energy from the incident light so that the electron occupies vacant positions in the energy levels, the transition is not accompanied by radiation. (MBD/ SiO_2) compound has a large permeability and its electrons are bound by covalent bonds, so it needs a high electron energy to move to higher energy levels. [81] The previous figure for the studied samples shows that the transmittance spectrum of the pure sample is higher than that of the anesthetized samples and the lowest absorption rate at the highest percentage of doping of silicon oxide and at the percentage of doping 0.01,0.03, 0.05(gm) the

transmittance spectrum is almost the same, with a clear decrease in the same thing at 600 nm Approximately.

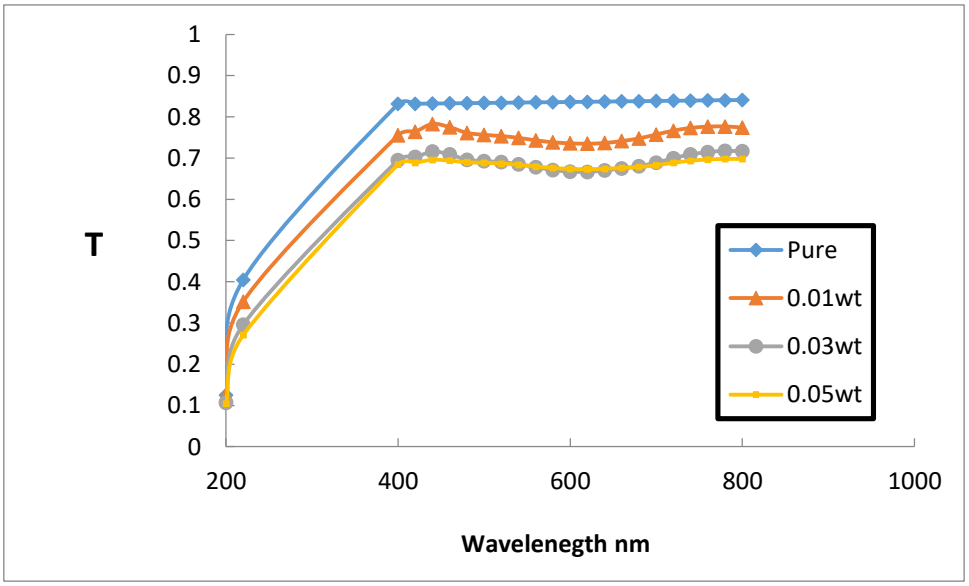

Figure (4.3): The transmittance spectra as function of wavelength λ(nm) of (MBD/ SiO_2) nanocomposite film at deffent value of Sio_2

.

4.3.3 Absorption Coefficient (α)

Fig (4.4) shows α as a function the wavelength of the nanocomposites (MBD/ SiO_2) It is observed that the absorption coefficient decreases at the high wavelength, so the probability of electron transfer is small as the energy of the photon is small so that the electron can move between the bands [82].

The higher energy, the α is higher; This means there is high potential of electron transitions and therefore, the energy of the incident photon is sufficient to move the electron between the valence and conduction bands. The energy of a photon is greater than the energy of the forbidden field, and This means that the absorption coefficient reveals the nature of electron transfer from valence band region BV to conduction band region BC [82]. We are observed that absorption values are high at high energies, so the energy of incident photon is good for direct electron transfer, while at low energies the electron cannot cross the

restricted energy gap and move from valence band to conduction band, direct electron transfer from the valence band to the conduction band occurs at values of the absorption is greater than 10^{-4} cm^{-1}, while the indirect transport is at absorption values less than 10^{-4} cm^{-1}. The means that electron transfer is indirect for MBD compound doped with SiO_2 nanoparticles because the absorption coefficient values are less than 10^{-4} cm^{-1}. We note that the values of the absorption coefficient increase with the increase of the doping ratios, especially at high energies, and we also note that the change in absorption coefficient with photon energy be little at low energies and then changes quickly and significantly near the edge of the optical absorption. As it is clear from all the curves that there is an absorption region $\alpha<10^4$ cm^{-1} and this probably does not occur directly electronic transitions, as we notice that the absorption edges shift slightly towards low photon energy and this effect is called (Burstien-Moss) This is due to generation of donor levels within band gap near conduction band, and this resulted in the absorption of low-energy photons and, thus, an apparent appearance. Increase in absorption coefficient values [83].

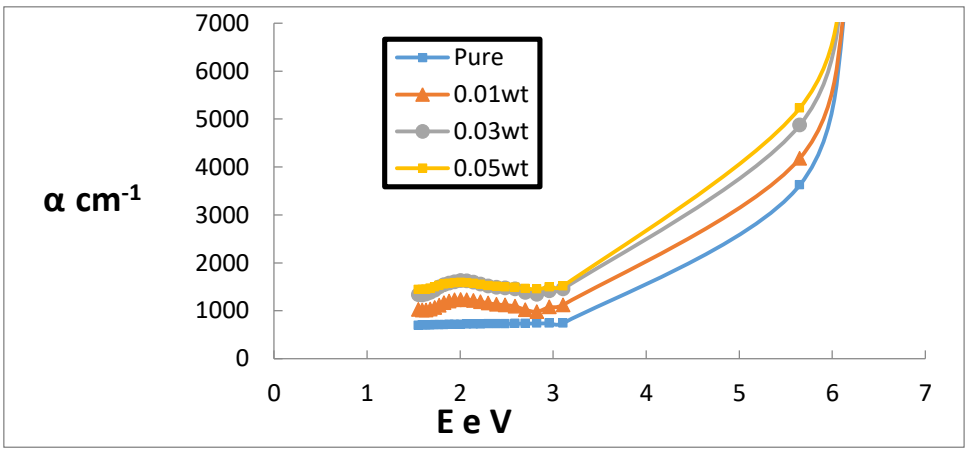

Figure (4.4): Variations of absorption coefficient in terms of photon energy for (MBD: SiO_2) nanocomposites.

4.3.4 Energy band gaps of allowed & forbidden direct Transition

A permissible & forbidden energy band gap in the indirect transition band was calculated using the equation (2-16). The value of exponent (r) depends on

the nature of transitions. In permissible direct transformations, its value is 1/2. In the case of forbidden direct transformations, its value is 2/3, and value the energy gap E_g corresponding to direct electronic transitions is graphically determined from the graph of the graph of (αhυ) m changes in terms of (hυ) then the best and furthest linear part of the curve is taken and plotted as a straight-line tangent to it. So that corresponds the intersection of this tangent with the horizontal axis (hυ) with the value of the energy gap E_g, becomes (αhυ) m = 0. The figure (4.5), (4.6) represents energy gap of films in allowed and forbidden direct electronic transitions. It is noted that the values are listed of Table (4.1) and it can see that the energy gap values decrease by increasing weight ratios in SiO_2. This is attributed to creation of site levels in forbidden energy gap; The transition of case carried out of two stages involving transition of electron from VB to local levels to CB due to the increase in weight percentage of SiO_2 nanoparticles [84]. The behavior is attributed to fact the nano -composites are of a hetero-geneous type (i.e., electronic conduction depends on the additional condensation), and increase of SiO_2 and nano particles provides electronic pathways in methyl blue dye facilitating the electron transit from VB to CB, which explains decrease the Eg with increase SiO_2 [78].

In Figure 4-6, it is observed that when the ratios of SiO_2 nano doping increases, the energy gap values decrease, and the electrons can move from VB to CB easily with high drug ratios.

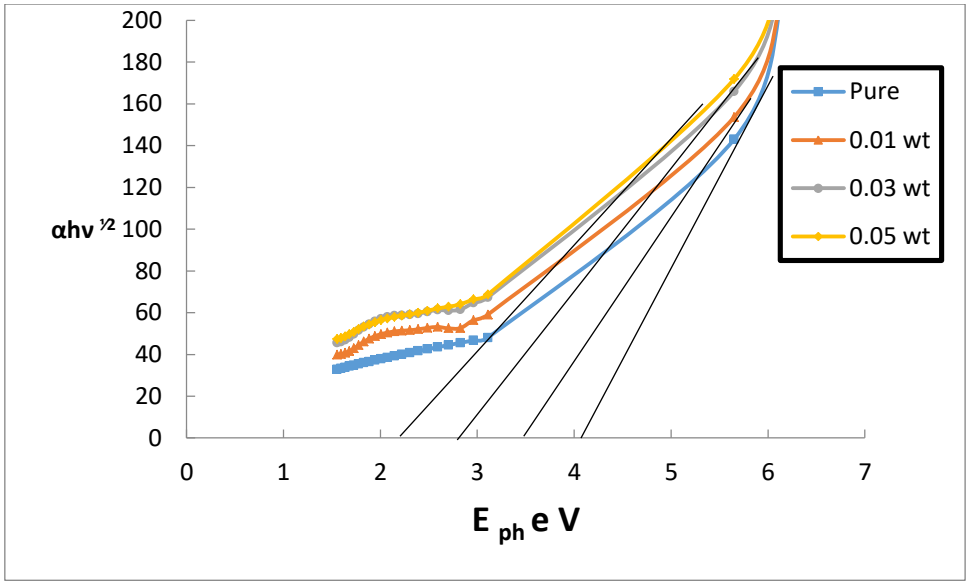

Figure (4.5): The variation $(\alpha h\upsilon)^{1/2}$ by photon energy for (MBD: SiO_2) nanocomposites.

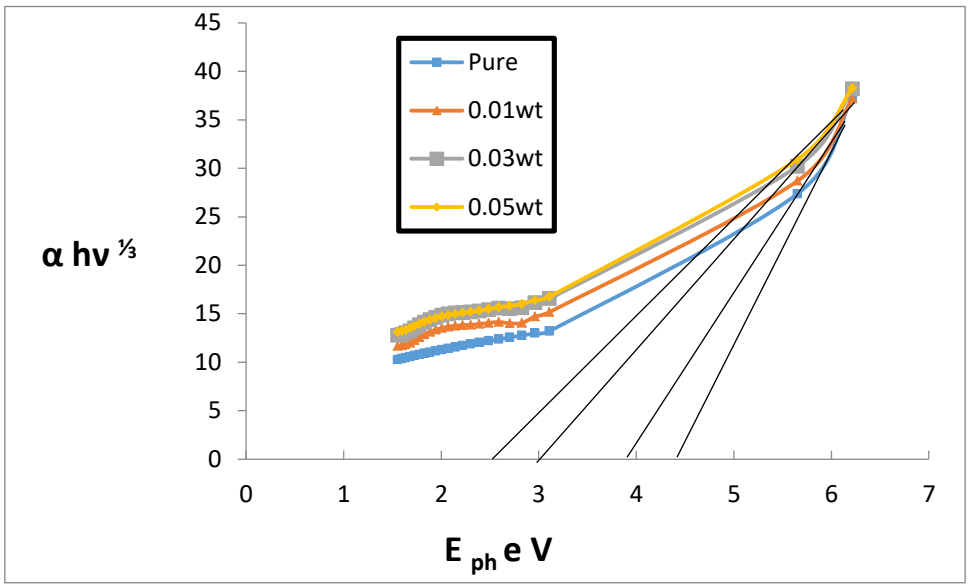

Figure (4.6): The variation $(\alpha h\upsilon)^{1/3}$ by photon energy for (MBD: SiO_2) nanocomposites.

Table (4.1): shows the energy gap values of permissible and forbidden direct transitions of the samples.

Sample	Permissible energy gap (ev)	forbidden energy gap (ev)
Pure	4.1	4.50
0.01	3.52	4.1
0.03	2.8	3.10
0.05	2.2	2.5

4.3.5 Refractive Index (n)

The reflection formula is given for the semiconductor in the case of orthogonal fall Knowing that the reflectivity on the inner surface of the samples is negligible from formula (2.8)

Figure (4.7) shows change n of nano-composites (MBD/SiO_2) as function of wavelength. It is clear this fig that refractive index increases by increasing concentration of (silicon oxide) in the methyl blue dye. The reason for this result is that increasing the concentration of (silicon dioxide) leads of an increase in density of nanocomposites [79,85,86].

The value of the doping ratio due to transmitting the largest wavelength is greater while decreasing at the larger wavelength.

A small peak appears at ~600 nm, in a pure sample the spectrum is nearly linear. The refractive index curve of all samples except the pure sample increases slightly with increasing wavelength (abnormal dispersion), and it is known that behavior of n curve is almost similar of nature of reflectivity due to the correlation of R with n in addition, the decrease in the values of n at a wavelength greater than 600 nm is due to lower absorption [87].

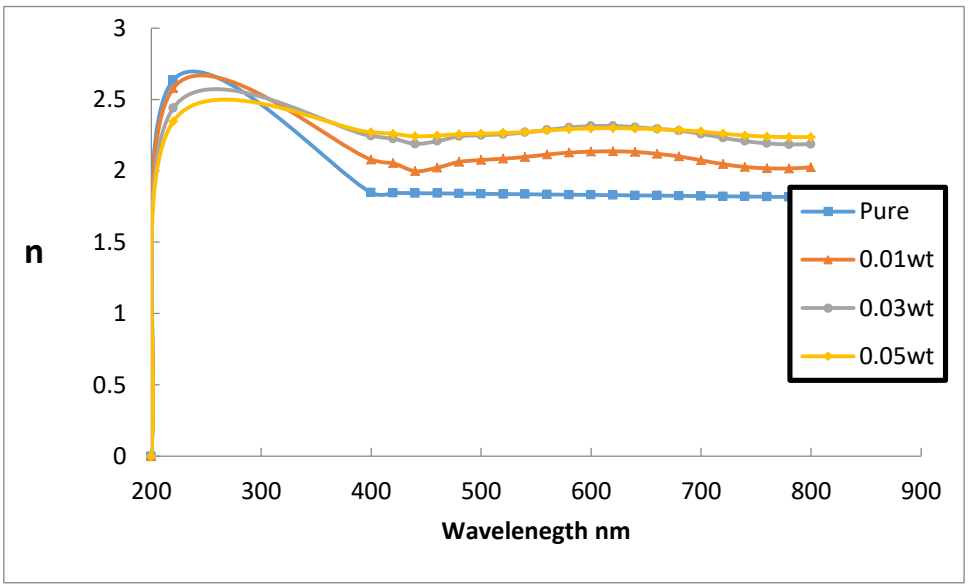

Figure (4.7): The refractive index (n) as function of wavelength for (MBD:SiO2).

4.3.6 Extinction Coefficient (k_0)

Figure (4.8) shows change of K_0 by function of wavelength, for (MBD/SiO_2). It can see (k_0) has low value of low concentration, but it increases by increasing concentration (SiO_2). It is attributed the increase in the **α** with increase in wt ratios (SiO_2). The K_0 has high values in the UV, and this behavior is related by high absorption of nanocomposite's samples. the k_0 of nanocomposites increases by the increase of λ in the vis and near-IR regions which is related to the **α** of nanocomposites which is nearly constant in the vis & near-IR region, thus, k_0 increases by increasing wavelength [88,89]

It was observed that the values of K_0 increase with increase in doping ratios SiO_2 nanoparticles and therefore increase in values of absorption coefficient with the increase in the ratios of the doping added to the membranes, and the extinction coefficient also increases with the long duration. [90]

The spectra of the extinction coefficient increase with the increase of the doping ratios and is almost linear in the net sample, we found that the values of (k_0) are

small in the case of low wavelengths and then start to increase and this indicates an increase in the absorption values and therefore the absorption coefficient increases and the damping coefficient increases.

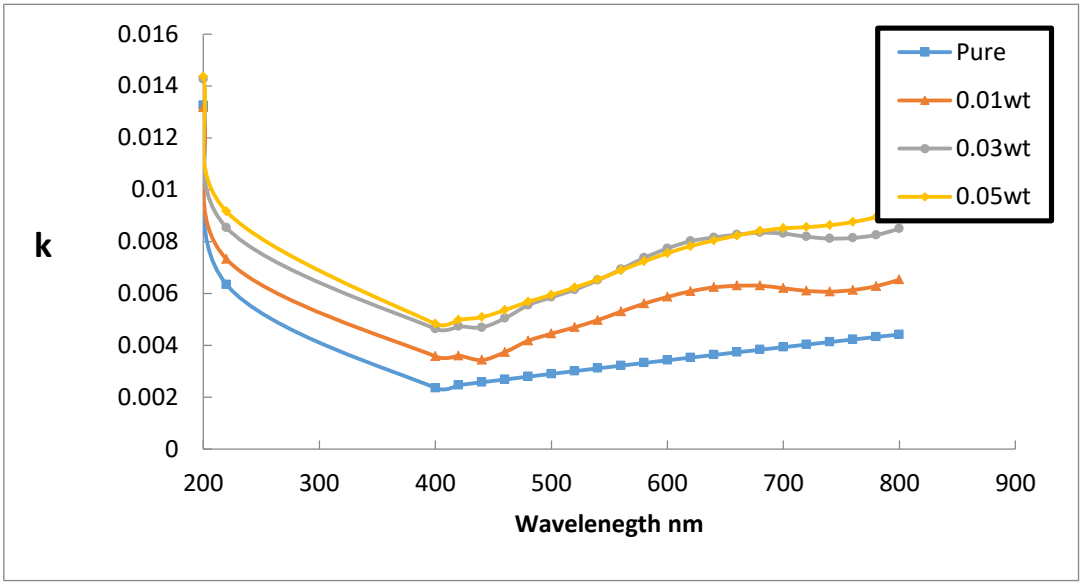

Figure (4.8): Changes of extinction coefficient with wavelength λ(nm) for samples (MBD:SiO_2) nanocomposites.

4.3.7 Dielectric Constants

The constant of parts real - imaginary was calculated to the nanocomposites (MBD/SiO_2). High dielectric values compared to the dielectric values. The real value of the dielectric is based on the values of n^2, k^2, while the imaginary dielectric is based on the values of n, k.

Figures (4.9) and (4.10) show the change in the dielectric constant of two parts (real - imaginary) as function of λ. These figures show that the constant of real and imaginary two fractions increase by increasing concentrations SiO_2 nanocomposites, and this behavior is related to increase electric polar-ization because the input nanoparticle concentration of sample, that is, the increase in di-electric const for (MBD/SiO_2) partially increases in the charges within the methyl blue pigment [91]. The di-electric const depending on n because effect of K_0 is small and imaging part of di-electric const related to K in the vis &

near-IR of λ h where the refractive index is nearly constant while the extinction coefficient increases with increasing wavelength. [92].

It is clear from the true dielectric constant curves (4.9) that they are similar to the refractive index curves in (4.7) in which the effect of the extinction coefficient is weak.

As for (4.10), it displays the spectra of the dummy dielectric constant of the movement of the electrodes causing the energy loss, and we note that the increase in impurities increases ε_i and they are very similar when the damping ratios are (0.01, 0.03, 0.05).

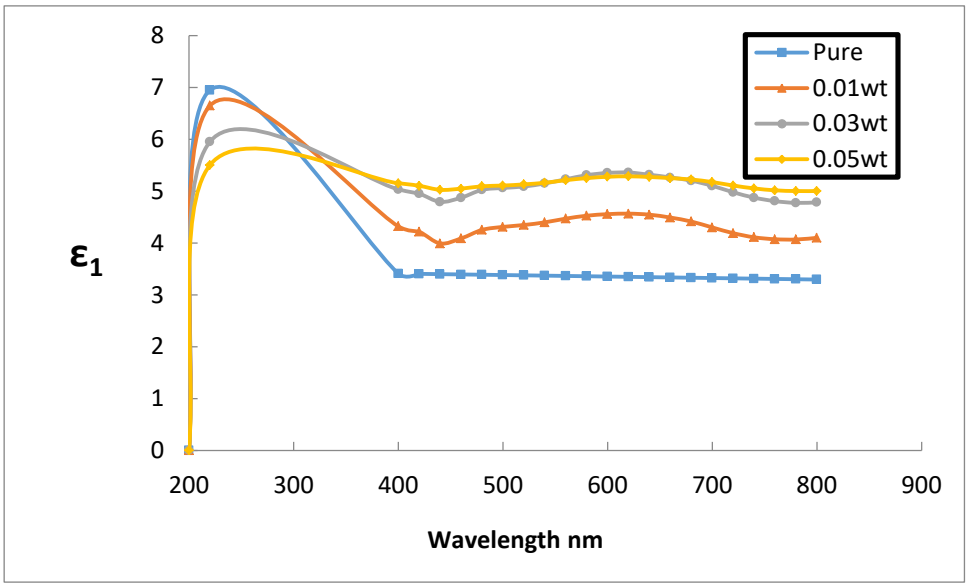

Figure (4.9): The real di-electric const (ε_1) as a function of incident λ for (MBD: SiO_2).

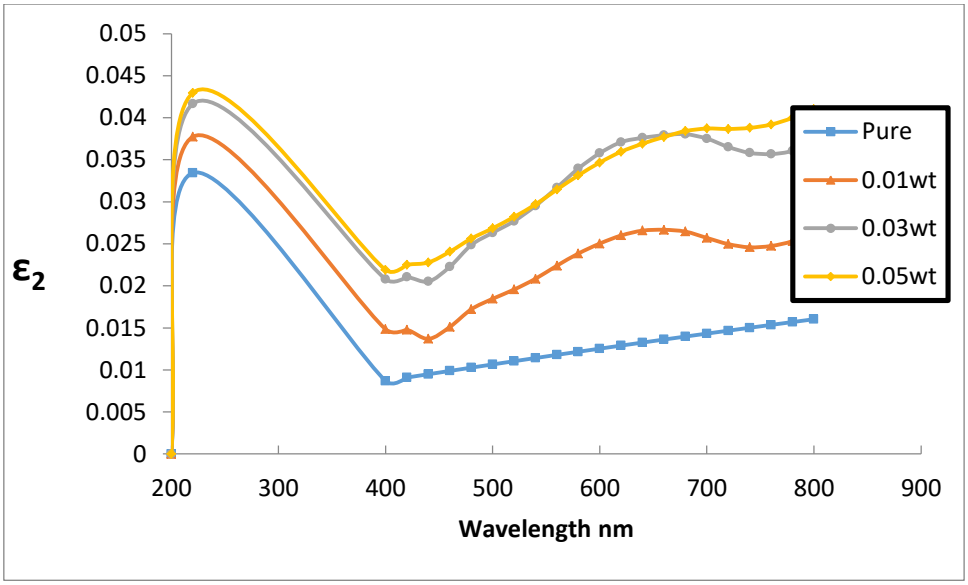

Figure (4.10): The imaginary di-electric const (ε_2) as a function of λ (MBD: SiO_2).

4.3.8 Optical Conductivity (σ_{op})

Figure (4.11) shows change the photoconductivity as function of λ of nanocomposites ($MBD_/SiO_2$). Where the increase in optical conductivity is because of increase charge carriers. spectra for photoconductivity increases when the doping ratio increases, noting that the two spectra for the doping ratios are 0.01,0.03, 0.05(gm) are almost the same, the behavior of the photoconductivity is similar to that of the absorption coefficient α because the relationship between σ and α is a direct relationship and this is due to the fact that as the material absorbs light, the majority and minority charge carriers activate the movement and therefore their number increases.

The increased photoconductivity at the lower photon wavelength is due to the higher absorption of all nanocomposite's samples in this region, and thus the increased charge transfer excitation. photoconductivity of nanocomposites increases by increasing of SiO_2 nanoparticles, and behavior is led to the establishment for localized levels in Eg; Increasing concentrations SiO_2 increases density the localized phases in band structure, thus increasing α and thus increasing σ the (MBD/ SiO_2). [80,92].

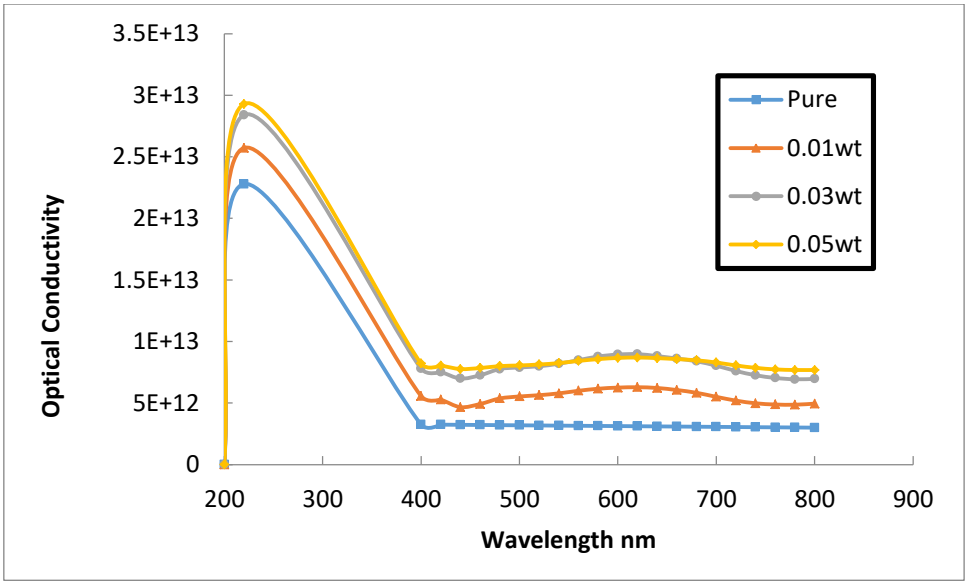

Figure (4-11): Optical conductivity as function by wavelength for (MBD: SiO_2) nanocomposites.

4.4 The Nonlinear Optical Properties

The nonlinear study of optical proper-ties was done in four different cases of the compounds (MBD/ SiO_2), the first case was a pure sample without addition of nanoparticles (SiO_2), while the other cases were the addition of nanoparticles (SiO_2) with difference. concentrations. We obtained the n and the nonlinear α from the nonlinear optic measurements at 540 nm wavelength of the dual laser in both cases Z scan closed-open aperture data for the samples with CW laser at (540 nm).

4.4.1 Non-linear Refractive Index Results

The non-linear reflection coefficient of four types has been studied. All these four states of the nanocomposite's films Measured using closed aperture Z scanning technology. Figure (4.12) shows closed slit z- scan for the first type, for the (MBD/ SiO2) without nanoparticles (SiO_2) and the other three bags with (0.01,0.03,0.05) (gm) added.

Figure (4.12) The figure shows the standard vectors of Z-Scan measurements in terms of distance. The peak of the valley transmittance curve that we obtained

from the closed aperture Z-scan data shows that the nonlinear refraction signal is negative ($n_2 < 0$), which leads to distortion of the focus of the lens in these samples [93].

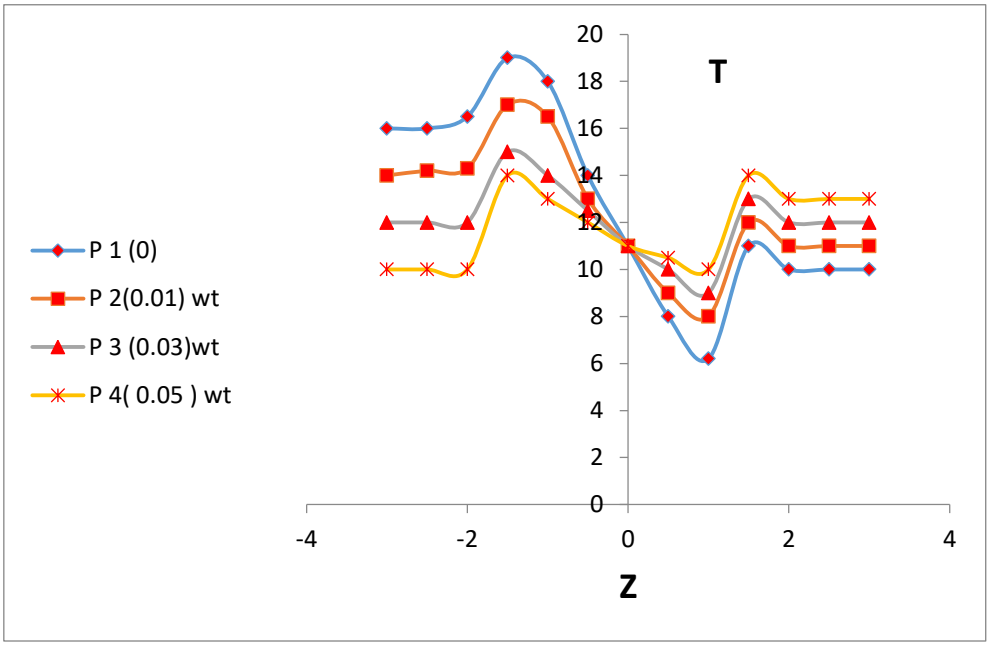

Figure (4.12): Closed-Aperture for the methylene blue dye doped SiO_2 films.

The order to describe behavior of the Z-Scan in previous fig, when sample are moves away from focus, The transmittance is constant, the transmit beam intensity is low, and when the sample approaches the focus of the beam The intensity of the transmitted beam is low and the transmittance remains relatively constant. When the sample approaches the focus of the beam, the intensity increases, resulting in the subjective lens in sample

tending of collect the beam that is located in the aperture is in the farthest field and therefore the transmittance that was measured in the place of the iris. And if the beam meets a non-linear shift in phase due to the sample and it is translated by the focal area and here part of the light that falls on the detector will change and the reason for that is the subjective lens that is generated within the material by condensation The laser beam and here the measured signal will appear in the

form of a crest and a valley and depends on the location of the crest and valley (Tp-v) on a non-linear phase shift signal. Moving within the nonlinear medium, the induced phase displacement is either negative or positive when the medium is non-self-centered or self-centered, respectively. We can determine the magnitude of the phase shift from the change in optical transmittance between the top and bottom. Outside the focal plane, increasing the defocus increases the beam spacing, this expands the beam at focus and will reduce the measured transmittance. Out of focus ($z > 0$), also the nonlinear birefringence is low and therefore the transmittance of Z is not independent [94,95].

4.4.2 Non-linear Absorption Coefficient Results

The non-linear absorption coefficient (β) of their first state (MBD) thin films (MBD) without nanoparticles (SiO_2) and the other three bags with the addition of (0.01,0.03,0.05) gm. of nanoparticles (SiO_2), can be measured by implementing the open-slit Z-Scan technology. The per-formed open aperture measurement scan shows an excessive amount of transmission around the focus of the lens.

The transmittance behaves linearly for different distances in the far field of the sample position (-Z). Then the transmittance decreases in the near field until the minimum value (T_{min}) is reached at Z = 0 for sample position (+Z). The intensity changes here and the reason is when the sample is moved within the center of the sample due to the absorption of two photons. The open aperture Z-Scan determines the change in transmittance values which are used to determine the absorption coefficient and that matches well [95,96]. Z-scanning with open aperture of (MBD/SiO_2) nano films at 540 nm, 5 mW shown in Figure (4.13) [95,96].

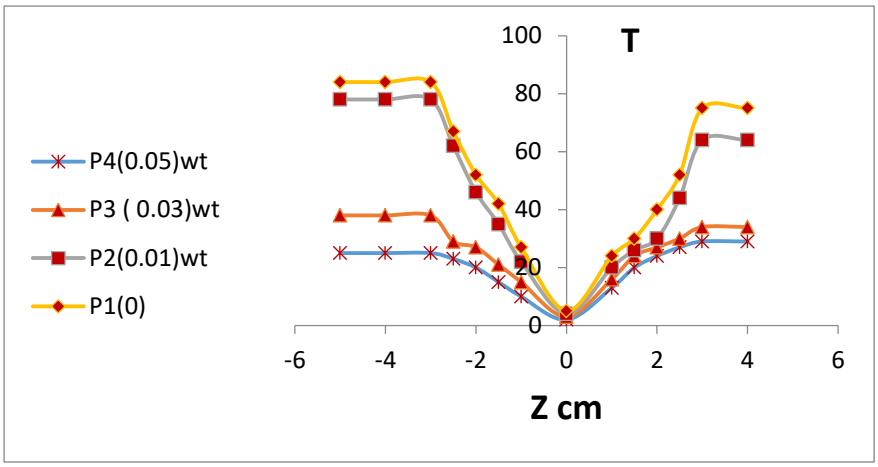

Figure (4.13): Open-Aperture for the methylene blue dye doped SiO_2 films [95,96]

While the phenomenon (saturated absorption) of open aperture Z-scanning is observed for a pure sample as shown in Figure (4.13), The transmittance behaves linearly in the far field at the location of the sample (+Z). In the near field, the transmittance curve increases until it reaches a maximum value (T_{max}) at Z = 0. The transmittance behaves linearly as it decreases at the position (-Z). The optical transmittance is sensitive to linear absorption. The saturation absorption changes the intensity during the transfer of the sample [96]. The density is greater within the crystal plane, and it has been observed that the largest nonlinear absorption is within a far radial field where the beam intensity is very narrow and no nonlinear effect occurs. The symmetrical peak of β acts as a negative nonlinear absorption coefficient, which leads to the appearance of the sample as saturated. This behavior is consistent with [96,97]. Then the nonlinear absorption index and the nonlinear refractive index values were found for the (MBD/ SiO2) nanoparticles as summarized in Table (4.3).

Table (4.2): The results of nonlinear optical properties for the methylene blue dye doped SiO_2 films by Z- scan technique with CW laser at (540 nm).

Sample	*Wt % of SiO_2*	*$\Delta\Phi$*	*L_{eff}*	*$n_2 \times 10^{-6}$ (cm^2/m W)*	*B (cm/m W)*
P_1	0	0.534	0.0946	0.017	0.1085
P_2	1	0.801	0.1015	0.026	0.1133
P_3	3	1.201	0.1056	0.039	0.1288
P_4	5	1.708	0.1102	0.056	0.1379

4.5 Conclusions

The main conclusions obtained in the research:

1. The drip and wipe method are a good and easy way to obtain a thin film, as the measurements were taken at room temperature in addition, normal atmospheric pressure without the need for vacuum.
2. The impurity samples have good refractive index and dielectric constant, and they can also be used in applications with large n values.
3. It was also found that the transmittance decreases when the percentage of doping increases and therefore, the absorbance increases with the increase in the ratio at doping visible rays, which reached the highest peak at 600 nm almost.
4. The real dielectric constant curves behave similar to the refractive index because they are related to each other where the damping coefficient is weak.
5. On another hand, it was showing E_g decreases by increase in percentage of doping, and this in-crease led to the declinate of the absorption edges towards lower energies, that is, a decrease in the concentration of charge carriers.

6. The results showed an improvement in most of the optical properties of the nanocomposites (MBD/SiO_2) with increasing the concentration of SiO_2 nanoparticles.
7. The results of closed-aperture Z-Scan for all cases show high nonlinear optical properties, self-defocusing negative.

4.6 Future Works

We recommend future work

1. We recommend the linear and nonlinear study of optical properties by Z-Scan technology for different types nanocomposites with new solvent, with lasers at different wavelengths and different power.
2. Using different nanomaterials with methyl blue dye and studying the spectral range and optical limit such as gold nanoparticles.
3. Use another type of pigment and use different methods to create another type of functional group in organic dyes.
4. Prepare dye membranes with various other materials and study their optical and electrical properties.

References

[1] Abdul Kader Jazmatia, Bassam Abdallah"Optical and Structural Study of ZnO Thin Films Deposited by RF Magnetron Sputtering at Different Thicknesses: A Comparison with Single Crystal, Materials Research", **(2017).**

[2] Al-Awadi**,** S. S. M. Chemical reduction synthesis of metallic nanoparticales doped with xanthen dye, spectroscopic study. Ph. D Thesis Department of Physics, College of Science University of Baghdad, Iraq (**2013**),

[3] B. Abd-Alkareem, "Effect of Nano-Copper Oxide on the Electrical and Optical Properties of (PMMA) Polymer", M.Sc. thesis, College of Education for pure sciences, University of Babylon, **(2016).**

[4] B. H. Rabee, M. A. Habeeb and A. Hashim, "Preparation of (PS-PMMA-$ZnCl_2$) Composites and Study their Electrical and Optical Properties", International Journal of Science and Research, Vol.3, No.10, **(2014).**

[5] Bahae, M. S. and Hassaibeak, M. P. *Handbook of Optics IV*, McGraw-Hill, Boston (**2000)**.

[6] Bahae, M. S. Said, A. A. Wel, T. Hagan, D. J. and Van, E. W**.**. Sensitive Measurement of Optical Nonlinearities Using a Single Beam. *IEEE Journal of Quantum Electronic,* 26(4). **(1990).**

[7] E. M. Abdelrazek, A.M. Abdelghany and A. E. Tarabih, "Characterization and Physical Properties of Silver/PVA nano- composite, Research Journal of Pharmaceutical", Biological and Chemical Sciences,Vol. 3, **(2012).**

[8] E. Saievar, Z. Dehghani, and M. Nadafan, ″Nonlinear Optical Properties of Nematic Liquid Crystal Doped with Differen Compositional Percentage of Synthesis of Fe3O4 Nanoparticles″, Journal of Molecular Liquids, Vol.190, **(2014).**

[9] E. Shahriari, M. Moradi & M. G. Varnamkhast "Investigation of nonlinear optical properties of Ag nanoparticles ", International Journal of Optics and Photonics, 9(2), **(2015).**

[10] F. L. Rashid, A. Hashim, M. A. Habeeb, S. R. Salman and H. Ahmed, "Preparation of (PS-PMMA) Copolymer and Study the Effect of Sodium Fluoride on Its Optical Properties", Chemistry and Materials Research, Vol.3, No.7. **(2013).**

[11] Filho, E. L. F. Araujo, C. B. D. and Rodrigues, JR. J. J.**.** High-order nonlinearities of aqueous colloids containing silver nanoparticles. *Journal of the Optical Society of America B*, 24(12). **(2007).**

[12] G. A. AL-Dahash, H. N. Najeeb, A. Baqer and R. Tiama, "The Effect of Bismuth Oxide Bi2O3 on Some Optical Properties of Poly vinyl Alcohol", British Journal of Science, Vol.4, pp.117-124, **(2012).**

[13] G. Svetlana, "Nonlinear Absorption and Refraction of Linearly Polarized Nanoseco nd Laser Radiation by Liquid Crystals in The Transient Regime", Conference on third order nonlinear optical materials, SPIE, Vol.3796, No.277, **(1999).**

[14] G. Svetlana, "Nonlinear Optical Response of Cyanobiphenyl Liquid Crystals to High-Power, Nanosecond Laser Radiation", Journal of Nonlinear Optical Physics & Materials, Vol. 9, No.3, **(2000).**

[15] Gamernyk, R. Periv, M. and Malynych, S. Nonlinear-optical refraction of silver nanoparticle composites. *Optica Applicata,* 44 (3), pp: 389-398. **(2014).**

[16] Ganeev, R. A. Ryasnyanskii, A.I. Kamalov, S. R Kodirov, M. K. and Usmanov, T. Nonlinear optical parameters of colloidal silver at various stages of aggregation. *Technical Physics,* **(2002).**

[17] Saudi Center for Nanotechnology: www.saudicnt.org.

[18] IbrahimKhan, KhalidSaeed, IdreesKhan; Nanoparticles: Properties, applications and toxicities, Arabian Journal of Chemistry (2019) 12, 908–931. , **(2019)**.

[19] Poole, C. P. and Owens, F. J. Introduction to Nanotechnology, John

Wiley & Sons, Inc., Hoboken, New Jersey, **(2003).**

[20] Faraday, M. Philos. Trans. Roy. Soc. (London) 147, ,145. **(1857).**

[21] Kubo, R., J. Phys. Soc. Jpn., 17, 975. **(1962).**

[22] Alhushan, Mansour, Alrashed, Maher; What do you know about nanotechnology? Nano Magazine, King Abdullah Institute for Nanotechnology, V.1, P.14-47. **(2008).**

[23] Shandiza, M. A., Journal of Physics and Chemistry of Solids. Vol.68, ,1396-1399. **(2007).**

[24] G. Svetlana, "Nonlinear Absorption and Refraction of Linearly Polarized Nanoseco nd Laser Radiation by Liquid Crystals in The Transient Regime", Conference on third order nonlinear optical materials, SPIE, Vol.3796, No.277, **(1999).**

[25] Ito T, Kobayashi K. A survey of in vivo photodynamic activity of xanthenes, thiazines, and acridines in yeast cells. Photochem Photobiol, 26:581–587.
doi:10.1111/j.1751-1097. 1977.tb07536.x**, (1977).**

[26] Epe B, Mützel P, Adam W DNA damage by oxygen radicals and excited state species: a comparative study using enzymatic probes in vitro. Chem Biol Interact, 67:149–165. doi:10.1016/0009-2797(88)90094-4 PMID:2844422, **(1988).**

[27] H. Hakim, N. Al- Garah and A. Hashim, "The Effect of Aluminum Oxide Nanoparticles on Optical Properties of (Polyvinyl Alcohol-Polyethylene glycol) Blend", Journal of Industrial Engineering Research, Vol.1, pp.94-98, **(2015).**

[28] Knowles A, Gurnani S A study of the methylene blue-sensitized oxidation of amino acids. Photochem Photobiol, 16:95–108. doi:10.1111/j.1751-1097.1972. tb07341.x PMID:5052681**, (1972).**

[29] H.N.Najeeb, " Study of Some Electrical and Optical Properties for Thin Films Prepared from Polymeric Composites ", M.Sc. thesis, College of sciences, University of Babylon, **(2011).**

[30] K. J. Kadhim, I. R.Agool and A. Hashim, "Enhancement in Optical Properties of (PVA-PEG-PVP)Blend By the Addition of Titanium OxideNanoparticles for Biological Application", Advances in Environmental Biology,Vol.10,pp.81-87, **(2016).**

[31] K. Khurana, A. K. Patel and K. Das,"Refractive Indices Studies on PVA and PVP Blends", International Journal for Scientific Research & Development, Vol. 4, **(2016).**

[32] Berneth H Azine dyes. In: Ullmann's Encyclopedia of Industrial Chemistry. Weinheim, Germany: Wiley-VCH Verlag GmbH & Co. KGaA, pp. 475–514. doi: 10.1002/14356007.a03_213.pub3, **(2008).**

[33] Ehrlich P Ueber das Methylenblau und seine klinisch-bakterioskopische Verwerthung. Z Klin Med, 2:710–713. [German] **(1881).**

[34] Oz M, Lorke DE, Hasan M, Petroianu GA Cellular and molecular actions of Methylene Blue in the nervous system. Med Res Rev, 31:93–117. doi:10.1002/med.20177 PMID:19760660**, (2011).**

[35] R.Ganeev , "Characterization of Nonlinear Optical Parameters of Polymethine Dyes " , Applied Physics B 76.6 , 683-686. **(2003).**

[36] Q. Mohammed, "Nonlinear optical and optical limiting properties of Chicago sky blue 6B doped PVA film at 633 nm and 532 nm studied using a continuous wave laser.", Modern Physics Letters B 22.16, 1589-1597, **(2009).**

[37] V. S. Sukmaran Kelly, K. L., Coronado, E. L., Lin, Z. and Schatz, G. C. **2003.** The optical properties of metal nanoparticles: the influence of size, shape, and dielectric environment. *Journal of Physical Chemistry B*, 107(3). **(2011)**.

[38] R. Manshad, and A. Hassa. "Nonlinear characterization of orcein solution and dye doped polymer film for application in optical limiting." Journal of Basrah Researches (Sciences), 38,4A**, (2012).**

[39] H. O. Seo Kreibig, U. and Vollmer, M. *Optical Properties of Metal Clusters*, Springer-Verlag, Heidelberg. **(2012).**

[40] R. Nandanwar, T. Wei, D. Hagan and E. Stryland, " Sensitive

Measurement of Optical Nonlinearities Using a Single Beam″, IEEE Journal of Quantum Electronics. Vol. 26. No. 4, **(2015)**.

[41] B. Ahmed, M. Dhami, T. S. and Rustagi, K. C. Nonlinear refraction in aqueous colloidal gold. *Optics Communications,* 133(1–6). **(2016).**

[42] M Rao Nadjari, H. and Azad, Z. A. Determining the nonlinear coefficient of gold and silver nano-colloids using SPM and CW Z-scan. *Optics and Laser Technology*, 44 (5). **(2018).**

[43] N. Shokoufi Mehendale, S. C. Mishra, S. R. Bindra, K. S. Laghate, M. Dhami, T. S. and Rustagi, K. C. Nonlinear refraction in aqueous colloidal gold. *Optics Communications*, 133(1–6). **(2019).**

[44] S. Wang Mercurochrome dye for Potential application in optical limiting ", Journal Optica Application, Vol.40. **(2020).**

[45] A. Awalludin P.N. Butcher and D. Cotter, "The Element of Nonlinear optics ", Cambridge UniversityPress, Cambridge, UK, **(2021).**

[46] C. Tara Rad, A. G. Abbasi, H. and Golyari, K. Fabrication and Nonlinear Refractive Index Measurement of Colloidal Silver Nanoparticles. *International Journal of Applied Physics and Mathematics*, 2(2). (**2022).**

[47] O. Ovchinnikov., refractive index dispersion and optical properties of dye doped polystyrene films, Malaysian Polymer Journal, Malaysia, Vol. 5, **(2022).**

[48] V. Lenart, G. Cruz, and S. Gomez, " Nonlinear Optical Refraction of The Dye-Doped E7 Thermotropic Liquid Crystal At The Nematic-Isotropic Phase Transition", cond- mat.soft., arxiv:1304.4537,pp.1-5, **(2013).**

[49] IbrahimKhan, KhalidSaeed, IdreesKhan; Nanoparticles: Properties, applications and toxicities, Arabian Journal of Chemistry 12, 908–931 , **(2019).**

[50] Mogilevsky, G., Hartman, O., Emmons, E.D., Balboa, A., DeCoste, J.B., Schindler, B.J., Iordanov, I., Karwacki, C.J. Bottom-upsynthesis of anatase nanoparticles with graphene domains. ACS Appl. Mater. Interfaces. 6, 10638–10648., **(2014).**

[51] J. I. Kroschwitz, "Electrical and Electronic Properties of Polymers", John Wiley and Sons, New York, **(1988).**

[52] S. Venkatachalam *, D. Mangalaraj, Sa.K. Narayandass,Structural, optical properties and VCNR mechanisms invacuum evaporated iodine doped ZnSe thin films **(2006).**

[53] Zaid A. Hasan, Effect Magneto – Optic on Ferromagnetic Nanoparticle Polymer Composite Films, NeuroQuantolo-gy; 19(6):25-29, **(2021).**

[54] TARIQ J.A., refractive index dispersion and optical properties of dye doped polystyrene films, Malaysian Poly-mer Journal, Malaysia, Vol. 5, 204-213, **(2010).**

[55] F-I-EZEMA Optical Characterization of Chemical Bath Deposited Bismuth Oxyiodide (BiOI) Thin Film **(2004).**

[56] KHALEEL R.I. et al, Effect of Doping Ni(etx)2 on Opti-cal Properties of Poly styrene, Al-Mustansiriyah Journal Sci., Iraq, Vol.22, No. 6, 129-136, **(2011).**

[57] F. Yakuphanoglu, M. Kanadaz, M. N. Yarasir, F.B. Senkal, - Electrical transport and optical properties of an organic semiconductor baswd on phthalocyanine, Physica B., Elsevier, 393, 235-238, **(2007).**

[58] M. Neghabi, A. Behjat, S.M.B. Ghorashi, S.M.A. Salehi, The effect of annealing on structural, electrical and optical properties of nano structured ZnS/Ag/ZnS films, **(2011).**

[59] ABDUL ZAHRA S., Effect of additive Al on the Optical properties of Polystyrene- Aluminum Composites, Ibn Al-Haitham Journal for Pure and Applli. Sci. Iraq, Vol.26(3), 111-120, **(2013).**

[60] J. H. Nahids, " Spectrophotmetric Analysis for the UV- Irradiated (PMMA) ", International Journal of Basic and Applied Sciences,12,2,58-67, **(2012).**

[61] Rebek, J.F, "Experimental Methods in Polymer Chemistry", John Wiley and Sons, New York, **(1980).**

[62] H.A. Macleod, "Thin Film Optical Filter", McGraw-Hill, New York. **(2001).**

[63] Mandau, A., Show, M.P. "The physics and Application of Amorphous Semiconductors", Academic press Inc., **(1986).**

[64] Mott, N.F., Davis, E.A. “Electronic processes in non-Crystalline Materials”, Clarendon press, 2dn Edition Oxford, **(1979).**

[65] R. Ali A. Jassim, M. Ali Habeb, "Effect of cobalt chloride (CoCl2) on the electrical and optical Properties of (PVA-PVP-CoCl2) films", Advances in Physics Theories and Applications, Vol.18, pp.47-53, **(2013).**

[66] D. Bag, H. Kramers, Quantum Mechanics. publisher Dover, NO, 9, p. 62, **(1957).**

[67] B.Snavely and J. Betteley. "Organic molecular photo physics”, Vol. 2.WileyInterscience, **(1973).**

[68] J. Alda, "Laser and Gaussian Beam Propagation and Transformation", Marcel Dekker.Inc,270,999-1013**,(2003).**

[69] C. Ostela, " Spectral-luminescent and lasing properties of laser active media

based on distyrylbenzene derivatives in various media", journal of Applied physics

,80, 6, 3167-3173, **(1996).**

[70] N. Jawad, " Non-linear Optical Studies of Liquid Crystal Materials Using ZScan Technique", M.Sc. Thesis, University of Babylon, **(2018).**

[71] W. Silfvast, "Laser Fundamentals", 2nd Edition, Cambridg University Press, **(2004).**

[72] G. Indebetouw," Nonlinear Optical Studies of Dye-Doped Nematic Liquid

Crystals", Ph.D. Thesis, Faculty of the Virginia Polytechnic Institute and State

University, Blacksburg, Virginia, **(2002).**

[73] L. Yong, and L. Dan, "Fabrication and Application of 1-D Micro-Cavity Film Made by Cholesteric Liquid Crystal and Reactive Mesogen”, Optical Materials Express 466, 6,2,691-696, (2016).

[74] M. L. Djeddou, influence de température de propriétés des couches minces d'oxyde de nickel dopé fer et élaboré par la technique spray pneumatique, Mémoire de magister, Université Med Khider Biskra, **(2017).**

[75] B. Abd-Alkareem, " Effect of Nano-Copper Oxide on the Electrical and Optical Properties of (PMMA) Polymer", M.Sc. thesis, College of Education for pure sciences, University of Babylon, **(2016).**

[76] E. M. Abdelrazek, A.M. Abdelghany and A. E. Tarabih, "Characterization and Physical Properties of Silver/PVA nano- composite, Research Journal of Pharmaceutical", Biological and Chemical Sciences,Vol. 3,pp.484-459, **(2012).**

[77] E. Shahriari, M. Moradi & M. G. Varnamkhast "Investigation of nonlinear optical properties of Ag nanoparticles ", International Journal of Optics and Photonics, 9(2), 107-114, **(2015).**

[78] F. L. Rashid, A. Hashim, M. A. Habeeb, S. R. Salman and H. Ahmed, "Preparation of (PS-PMMA) Copolymer and Study the Effect of Sodium Fluoride on Its Optical Properties", Chemistry and Materials Research, Vol.3, No.7, pp.55- 58, **(2013).**

[79] G. A. AL-Dahash, H. N. Najeeb, A. Baqer and R. Tiama, "The Effect of Bismuth Oxide Bi2O3 on Some Optical Properties of Poly vinyl Alcohol", British Journal of Science, Vol.4, pp.117-124, **(2012).**

[80] B. H. Rabee, M. A. Habeeb and A. Hashim, "Preparation of (PS-PMMA-ZnCl2) Composites and Study their Electrical and Optical Properties", International Journal of Science and Research, Vol.3, No.10, pp.1593-1596, **(2014)**.

[81] P.N. Butcher and D. Cotter, "The Element of Nonlinear optics ", Cambridge UniversityPress, Cambridge, UK, **(1990)**.

[82] K. J. Kadhim, I. R.Agool and A. Hashim ,"Enhancement in Optical Properties of (PVA-PEG-PVP)Blend By the Addition of Titanium OxideNanoparticles for Biological Application", Advances in Environmental Biology,Vol.10,pp.81-87, **(2016)**.

[83] Tariq J.A., refractive index dispersion and optical properties of dye doped polystyrene films, Malaysian Polymer Journal, Malaysia, Vol. 5, 204-213, **(2010)**.

[84] H. Hakim, N. Al- Garah and A. Hashim, "The Effect of Aluminum Oxide Nanoparticles on Optical Properties of (Polyvinyl Alcohol-Polyethylene glycol) Blend", Journal of Industrial Engineering Research, Vol.1, pp.94-98, **(2015)**.

[85] K. Khurana, A. K. Patel and K. Das,"Refractive Indices Studies on PVA and PVP Blends", International Journal for Scientific Research & Development, Vol. 4, **(2016)**.

[86] M. Abdelaziz and E.M. Abdelrazek,"Thermal-Optical Properties of Polymethylmethacrylate/Silver Nitrate Films", Journal of Electronic Materials, Vol.42, No.9, pp.2743-2751, **(2013)**.

[87] Abdul Kader Jazmatia, Bassam Abdallah"Optical and Structural Study of ZnO Thin Films Deposited by RF Magnetron Sputtering at Different Thicknesses: A Comparison with Single Crystal", Materials Research **(2017)**.

[88] E. M. Abdelrazek, A.M. Abdelghany and A. E. Tarabih, "Characterization and Physical Properties of Silver/PVA nano- composite, Research Journal of Pharmaceutical", Biological and Chemical Sciences,Vol. 3,pp.484-459, **(2012)**.

[89] H.N.Najeeb, " Study of Some Electrical and Optical Properties for Thin Films Prepared from Polymeric Composites ", M.Sc. thesis ,College of sciences, University of Babylon , **(2011)**.

[90] R.R. Krishnamurthy and R. Alkoudan, "Nonlinear characterization ofMercurochrome dye for Potential application in optical limiting ", Journal Optica Application, Vol.40, PP.127, **(2010)**.

[91] K. Khurana, A. K. Patel and K. Das,"Refractive Indices Studies on PVA and PVP Blends", International Journal for Scientific Research & Development, Vol. 4, **(2016)**.

[92] V. Lenart, G. Cruz, and S. Gomez," Nonlinear Optical Refraction of The Dye-Doped E7 Thermotropic Liquid Crystal At The Nematic-Isotropic Phase Transition", cond-mat.soft., arxiv:1304.4537,pp.1-5, **(2013)**.

[93] G. Svetlana, "Nonlinear Optical Response of Cyanobiphenyl Liquid Crystals to High-Power, Nanosecond Laser Radiation", Journal of Nonlinear Optical Physics & Materials, Vol. 9, No.3, pp. 365-411, **(2000)**.

[94] M. Bahae, A. Said, T. Wei, D. Hagan and E. Stryland, " Sensitive Measurement of Optical Nonlinearities Using a Single Beam", IEEE Journal of Quantum Electronics. Vol. 26. No. 4, pp.760-769, **(1990)**.

[95] E. Saievar, Z. Dehghani, and M. Nadafan, "Nonlinear Optical Properties of Nematic Liquid Crystal Doped with Differen Compositional Percentage of Synthesis of Fe3O4 Nanoparticles", Journal of Molecular Liquids, Vol.190, pp.6- 9, **(2014)**.

[96] G. Svetlana, "Nonlinear Absorption and Refraction of Linearly Polarized Nanoseco nd Laser Radiation by Liquid Crystals in The Transient Regime", Conference on third order nonlinear optical materials, SPIE, Vol.3796, No.277, pp.100-111, **(1999)**.

[97] Z. Xiaoqiang, W. Changshun and L. Zenga. "Nonlinear Optical Properties of a Series of Azobenzene Liquid-Crystalline Materials", Optik, Vol.123, pp.26–29, **(2012)**.

الخلاصة

تم تحضير المركبات النانوية (صبغة أزرق الميثيل: SiO2) بطريقة الصب بنسب وزنية مختلفة من الجسيمات النانوية (أكسيد السيليكون).

تمت دراسة الخصائص التركيبية والضوئية وغير الخطية للمركبات النانوية. تشمل الخصائص الهيكلية المجهر الضوئي. أظهرت نتائج الفحص بالصور المجهر الضوئي توزيع جزيئات أكسيد السيليكون النانوية داخل صبغة الميثيل الزرقاء لجميع أغشية المركبات النانوية، كما أظهرت صور المجهر الضوئي شبكة مستمرة من الأيونات داخل صبغة الميثيل الزرقاء بنسبة عالية من الجسيمات النانوية. أظهرت نتائج الخواص الضوئية للمركبات النانوية (SiO2/MBD) أن الامتصاصية ومعامل الامتصاص ومعامل الخمود ومعامل الانكسار وثوابت العزل الحقيقي والخيالي والتوصيل البصري تزداد مع زيادة تراكيز الجسيمات النانوية بينما كانت فجوة نطاق النفاذية والطاقة تنخفض مع زيادة تراكيز الجسيمات النانوية (SiO2). تتميز المركبات النانوية (SiO2/MBD) بامتصاص عالي في منطقة الأشعة فوق البنفسجية.

تم حساب الاختبارات اللاخطية باستخدام تقنية (Z–Scan) في حالتين (الفتحة المغلقة) و (الفتحة المفتوحة) للحصول على معامل معامل الانكسار اللاخطي (n_2) ومعامل الامتصاص اللاخطي (β). موجة (CW) بطول موجة (540 نانومتر). أظهرت النتائج انخفاضاً في كل من معامل معامل الانكسار اللاخطي ومعامل الامتصاص اللاخطي عند زيادة التركيزات لجميع عينات أغشية المركبات النانوية. أظهرت النتائج أن معامل الانكسار اللاخطي في جميع العينات سالب. لوحظ من نتائج معامل الامتصاص اللاخطي (β) في ثلاث حالات من الأغشية الرقيقة لمزيج (SiO_2/MBD) مع إضافة (1%،3%،5%) بالوزن من جسيم النانو (SiO_2) امتصاص الفوتونين بينما لوحظ أن أكبر امتصاص غير خطي (امتصاص مشبع) في حالة العينة نقية.

جمهورية العراق
وزارة التعليم العالي والبحث العلمي
جامعة بابل
كلية التربية للعلوم الصرفة
قسم الفيزياء

دراسة الخصائص الخطية واللاخطية لصبغة الميثايلين الزرقاء المطعمة بجسيمات SiO_2 النانوية

رسالة مقدمة
الى مجلس كلية التربية للعلوم الصرفة في جامعة بابل
وهي جزء من متطلبات نيل درجة الماجستير
في التربية / الفيزياء

من قبل الطالب

مها حسن نوري خليل

بكالوريوس تربية فيزياء
جامعة بابل 2010 م

بإشراف

البروفسور. د. زيد عبد الزهرة حسن الشمري

1444هـ **2022 م**